NANO-STRUCTURED TRIBOELECTRIC NANO GENERATORS FOR INTERNET-OF-THINGS (IOT) APPLICATIONS

by

Kemal Ünlü

B.S., Electrical and Electronics Engineering, Boğaziçi University, 2016

Submitted to the Institute for Graduate Studies in
Science and Engineering in partial fulfillment of
the requirements for the degree of
Master of Science

Graduate Program in Electrical and Electronics Engineering
Boğaziçi University
2018

NANO-STRUCTURED TRIBOELECTRIC NANO GENERATORS FOR INTERNET-OF-THINGS (IOT) APPLICATIONS

APPROVED BY:

Prof. Şenol Mutlu (Thesis Supervisor)	.....
Prof. Amitav Sanyal	.....
Assist. Prof. Hakan Doğan	.....

DATE OF APPROVAL: 17.09.2018

ACKNOWLEDGEMENTS

In these past two years of my graduate education, I have met many people who have supported me in all kinds of events and have great effort to complete this work.

The first person I want to mention is my supervisor Prof. Şenol Mutlu. I would like to thank him for I would like to thank him for leading me to this work, producing solutions in every point where I have problems, and conveying my valuable experience to me. working with him has been an invaluable experience for me and I will be grateful to him for my life.

I also would like to thank Prof. Amitav Sanyal and his student Dr. Tuğçe Nihal Gevrek for their cooperation in this work. The chemical processes that have to be applied in this study have been successfully implemented and delivered to me with their work. These efforts have a very important place in this thesis.

Another person I am grateful is Emre İşeri. In the short time we work together, he conveys me his experience and complete the microfabrication of steel electrode which used in this work.

I like to express my deepest gratitude to my colleagues, Dr. Gürkan Sönmez, Ozan Ertop, Ahmet Yasin Çelik and Doruk Dündar. During our working hours they offered me a warm friendship. They helped me to answer any questions I had on my mind.

Last but not least, I would like to thank Ayşenur. Although she cannot be around physically in the majority of this time, she made me feel her presence for every second. Her presence always support me and let me continue when I had bad times.

This work was financially supported by the TUBİTAK research grant 215E288.

ABSTRACT

NANO-STRUCTURED TRIBOELECTRIC NANO GENERATORS FOR INTERNET-OF-THINGS (IOT) APPLICATIONS

In this thesis, three different triboelectric energy harvesters were designed and manufactured. Polydimethylsiloxane (PDMS) was used as triboelectric surface in the first of these harvesters. In addition to untreated this surface, PDMS surfaces with polystyrene (PS) and poly(pentafluorostyrene) (PPFS) nano brushes are used and comparisons of these three have been made. The effective area of these three surfaces are 1 cm^2. In the measurements of the PDMS surface maximum transferred power is measured as 45.7 nW at 300 MΩ load. This value was increased by approximately 16 times for the PS sample to 750.6 nW and for the PPFS sample by 48 times to 2.3 μ W. Thus, it has been successfully shown that the nano brushing method seriously increases the triboelectric charge density. Polytetrafluoroethylene (PTFE) film and steel electrode were used for the other harvesters fabricated. In the first of the PTFE-based harvesters, the steel film passed through the microfabrication process. In the measurements of this harvester with 1 cm^2 effective area, maximum transferred power is measured as 895 nW at 250 MΩ load. This harvester which is designed as keyboard button shows that the batteryless keyboard can be made by using triboelectric energy harvesters. The effective area of the last harvester fabricated in macro size is 60 cm^2. The maximum transferred power with this harvester is measured as 203 μW at 140 MΩ. This generated power succesfully lit up 196 commercial LED. It has also been shown that this power can be used in IoT applications that use low power bluetooth.

ÖZET

NESNELERİN İNTERNETİ (IOT) UYGULAMALARI İÇİN NANO YAPILI TRİBOELEKTRİK NANO JENARATÖRLER

Bu tezde, üç farklı triboelektrik enerji hasatlayıcısı tasarlanıp üretilmiştir. Bu hasatlayıcılardan ilkinde triboelektrik yüzey olarak polidimetilsiloksan (PDMS) kullanılmıştır. Daha sonra işlem görmemiş bu yüzeyin yanında polistiren (PS) ve poli (pentaflorostiren) (PPFS) nano fırçalı PDMS yüzeyler kullanılarak bu üçünün karşılaştırılmaları yapılmıştır. Bu üç yüzeyde efektif olarak kullanılan alan 1 cm^2'dir. PDMS yüzey ile yapılan ölçümlerde maksimum aktarılan güç 300 MΩ yük değerinde 45.7 nW olarak ölçülmüştür. Bu değer PS örneğinde yaklaşık 16 kat artarak 750.6 nW, PPFS örneğinde ise 48 kat artarak 2.3 μW olarak ölçülmüştür. Böylece nano fırçalama yönteminin triboelektrik yük yoğunluğunu ciddi bir şekilde arttırdığı başarıyla gösterilmiştir. Üretilen diğer hasatlayıcılarda politetrafloretilen (PTFE) filmi ile çelik elektrot kullanılmıştır. PTFE kullanılan hasatlayıcıların ilkinde çelik film mikrofabrikasyon işleminden geçmiştir. 1 cm^2 efektif alanı olan bu hasatlayıcı ile yapılan ölçümlerde maksimum aktarılan güç 250 MΩ yük değerinde 895 nW olarak ölçülmüştür. Klavye butonu şeklinde tasarlanan bu hasatlayıcı ile triboelektrik enerji hasatlayıcıları ile pilsiz bir klavye yapılabileceği gösterilmiştir. Makro boyutlarda üretilen son hasatlayıcının efektif alanı 60 cm^2'dir. Bu hasatlayıcı ile aktarılan maksimum güç 140 MΩ yük değerinde 203 μW olarak ölçülmüştür. Üretilen bu güçle 196 ticari LED başarıyla yakılmıştır. Ayrıca, bu gücün düşük enerjili bluetooth kullanan IoT uygulamalarında kullanılabileceği gösterilmiştir.

TABLE OF CONTENTS

ACKNOWLEDGEMENTS . . . iii
ABSTRACT . . . iv
ÖZET . . . v
LIST OF FIGURES . . . viii
LIST OF SYMBOLS . . . xii
LIST OF ACRONYMS/ABBREVIATIONS . . . xiii
1. INTRODUCTION . . . 1
1.1. Triboelectric Effect . . . 5
1.2. Motivation and Novelty . . . 8
1.3. Outline of the Thesis . . . 9
2. THEORY . . . 10
2.1. Triboelectric Nano Generator . . . 10
2.2. Mathematical Modeling . . . 11
3. FABRICATION . . . 14
3.1. Fabrication of TENG with Nano Structured Polymer Surfaces . . . 14
3.2. Fabrication of TENG with Microfabricated Steel Electrode . . . 22
3.3. Fabrication of Macro Scale Triboelectric Generator . . . 24
4. CHARACTERIZATION MEASUREMENTS AND RESULTS . . . 27
4.1. Measurement Equipments . . . 27
4.1.1. Electrometer . . . 27
4.1.2. CNC Machine . . . 28
4.1.3. Load Connection Setup . . . 29
4.2. Measurements of TENG with Nano Structured Polymer Surfaces . . . 29
4.2.1. PDMS Measurement . . . 30
4.2.2. Polystyrene Measurement . . . 31
4.2.3. Poly(pentafluorostyrene) Measurement . . . 32
4.2.4. Comparison of the PDMS, PS and PPFS Measurement Results 33
4.2.5. LCD Application with Nano Structured TENG . . . 35
4.3. Measurements of TENG with Microfabricated Steel Electrode . . . 35

4.4. Measurements of Macro Scale Triboelectric Energy Harvester 37
4.4.1. Low Power Bluetooth Application 39
5. CONCLUSIONS AND FUTURE WORK 41
REFERENCES 43

LIST OF FIGURES

Figure 1.1. Electromagnetic Generator Example. 2

Figure 1.2. Three Different Type of Electrostatic Energy Harvester. 3

Figure 1.3. The Example of Piezoelectric Generator Model. 4

Figure 1.4. Wimshurst Machine and the Van de Graaff Generator with their discharge mechanism. 6

Figure 1.5. Triboelectric series. 7

Figure 2.1. TENG model. 11

Figure 3.1. PS nano brush growth with chemical methods on PDMS surfaces. 15

Figure 3.2. PPFS nano brush growth with chemical methods on PDMS surfaces. 16

Figure 3.3. General XPS spectra of PDMS, polystyrene and poly (pentafluorostyrene) coated PDMS (a) and high-resolution scanning of C1s regions (b). 17

Figure 3.4. FTIR spectra of PS, PPFS coated PDMS surfaces and untreated PDMS surface. 18

Figure 3.5. Comparison of ESEM images taken from the side sections of the surfaces. (a) RAFT agent coated PDMS-Al (5000x) (b) Polystyrene coated PDMS-Al (5000x). 19

Figure 3.6. Untreated, PS coated and PPFS coated PDMS surfaces. 19

Figure 3.7. Nano structured surfaces placed on a test setup. 20

Figure 3.8. The setup for bottom and top surfaces. 21

Figure 3.9. TENG with the nano structered polymer surface. 21

Figure 3.10. Keyboard button like design and crableg shaped steel electrode. . 22

Figure 3.11. Al coated PTFE film which is fixed and it's electrical contact is established. 23

Figure 3.12. TENG with microfabricated steel electrode. 24

Figure 3.13. Bottom part of the macro scale triboelectric generator. 25

Figure 3.14. Top part of the macro scale triboelectric generator. 26

Figure 3.15. Macro scale triboelectric generator. 26

Figure 4.1. Keysight B2985A Electrometer/High Resistance Meter. 27

Figure 4.2. CNC machine. 28

Figure 4.3. Load connection setup. 29

Figure 4.4. PDMS current measurement at 300 MΩ. 30

Figure 4.5. The instantaneous transferred power value for different load resistance for PDMS measurements. 30

Figure 4.6. PS current measurement at 300 MΩ. 31

Figure 4.7. The instantaneous transferred power value for different load resistance for PS measurements. 31

Figure 4.8. PPFS current measurement at 250 MΩ. 32

Figure 4.9. The instantaneous transferred power value for different load resistance for PPFS measurements. 32

Figure 4.10. Current values of PDMS, PS, and PPFS at 300 MΩ 250 MΩ. . . . 33

Figure 4.11. Transferred power values of PDMS, PS and PPFS for different load resistors. 34

Figure 4.12. The LCD application setup. (a) TENG is at seperation mode and (b) TENG is at contact mode. 35

Figure 4.13. The current measurement of TENG with microfabricated steel electrode at 250 MΩ. 36

Figure 4.14. The LCD application setup of TENG with microfabricated steel electrode. 36

Figure 4.15. Macro scale triboelectric energy harvester current measurement at 140 MΩ. 37

Figure 4.16. The instantaneous transferred power value for different load resistance for macro scale triboelectric harvester. 38

Figure 4.17. Driving LEDs with macro scale triboelectric generator. 38

Figure 4.18. TI-CC2650 Launchpad [23]. 39

LIST OF SYMBOLS

A	Surface area of triboelectric layer
Al	Aluminum
C	Carbon
CH3	Methane
C_{TENG}	Capacitance of triboelectric nano generator
d	Thickness of dielectric material
E_{air}	Electric field in air
E_p	Electric field in polymer
F	Flour
H	Hydrogen
O	Oxygen
OH	Hydroxyl
Q	Charge formed on electrodes of triboelectric generator
Si	Silicon
V	Potential difference
V_C	Potential difference of capacitor
V_{OC}	Open circuit potential difference
V_{TENG}	Potential difference of triboelectric nano generator
x(t)	Distance between triboelectric layers
ZnO	Zinc oxide
ϵ_0	Dielectric constant of air
ϵ_r	Dielectric constant of polymer
σ	Triboelectric surface charge density

LIST OF ACRONYMS/ABBREVIATIONS

3D	Three Dimensional
AIBN	Azobisisobutyronitrile
CNC	Computer Numerical Control
CVD	Chemical Vapor Deposition
ESEM	Environmental Scanning Electron Microscope
FTIR	Fourier Transform Infrared Spectroscopy
IC	Integrated Circuit
IOT	Internet Of Things
LCD	Liquid Crystal Display
LED	Light Emitting Diode
MEMS	Micro Electro Mechanical System
PDMS	Polydimethylsiloxane
PMMA	Poly(Methyl Methacrylate)
PPFS	Poly(Pentafluorostyrene)
PS	Polystyrene
PTFE	Polytetrafluoroethylene
PZT	Lead Zirconate Titanate
RAFT	Reversible Addition-Fragmentation Chain Transfer
RF	Radio Frequency
TENG	Triboelectric Nano Generator
THF	Tetrahydrofuran
XPS	X-ray Photoelectron Spectroscopy

1. INTRODUCTION

A technological development in the world in the last decades dramatically increase with the number of electronic devices. In addition to devices commonly used in daily life like phones, computers; many other personal electronic devices are developed and manufactured. The new areas like wearable electronics come to existence and the new products are introduced day by day. This exceeding increase in number of electronic devices is also cause huge increment for need of the power supply sources [1].

The traditional way of providing power supply to electronic devices is using batteries. Even though batteries are useful for relatively big and limited number devices; it has many disadvantages. First of all batteries are not clean energy sources. Because of this there must be very large scale recycling facilities for usage of the huge number of batteries. Even this difficult task achieved there will be a certain damage to environment.Secondly, batteries are not infinite sources, hence they must be replaced at regular intervals. It is not a tough task for a easily replaceable batteries. However, with the developing IC industry, the electronic devices more and more smaller, more commonly used, portable and wearable. Because of the spread of the electronic devices, simple assembly and accessibility, sustainability; wireless and self-powered battery-less systems are demanded for these devices. In order to fulfill this demand, various piezoelectric, thermal, photo voltaic, RF, electromagnetic, and electrostatic energy harvester are developed by using micro electromechanical systems (MEMS) process [2]. Beside the light and heat difference mechanical energy is the one of the biggest energy source to use. Especially, the usual daily low frequency movements, like the walking or the other movements of the humans, the opening or closing of the door, has the big potential to turning into electrical energy and satisfy the energy requirement of the wireless sensors which are needed for smart houses or internet of things applications frequently. Because of this potential there are different type of the harvesters manufactured which convert to mechanical energy to electrical energy. Electromagnetic, electrostatic and piezoelectric generators are the main mechanisms for self-powered systems [3].

Electromagnetic generators are often used for the energy harvesting. The technology behind these generators is well established and have found many application areas [4]. For MEMS applications, it is theoretically well-suited. Because it needs no initial energy input and it's voltage output is in range for MEMS applications. The example device manufactured with this technology is shown in Figure 1.1. Even tough it is commonly used technology it has difficulties to produce a solution for smaller products. Since, there is magnet usage, generators can not be reduced, the products are bulky and can not produce results in very low energy movements.

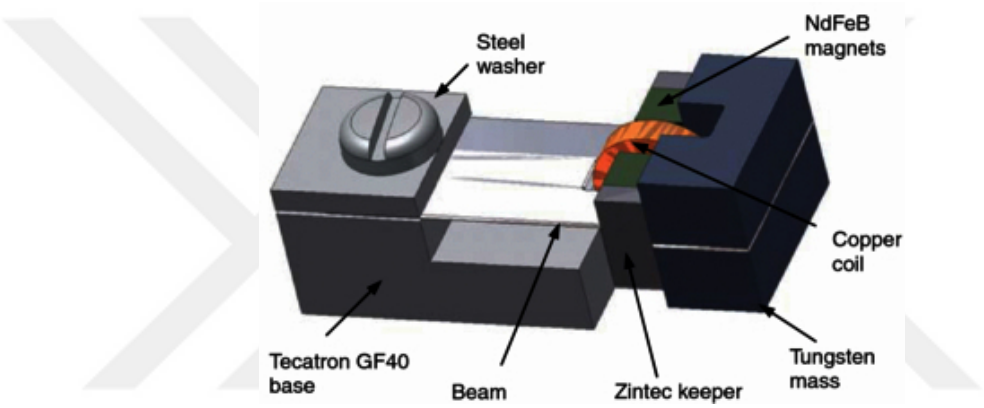

Figure 1.1. Electromagnetic Generator Example. [5]

Electrostatic energy harvesters are made of basically two movable electrically conductive electrode with a gap between them [6]. If the charge on the plate is kept constant, while distance between plate are changing the capacitance and the voltage change; and if the voltage is kept constant then with movement of the plates charges on the plates move, hence the current occurs. Electrostatic harvesters generate electrical energy from mechanical energy with these two methodologies. The main advantage of the electrostatic harvesters is excellent compatibility with integrated circuits in terms of micro systems [7]. the different three type of the electrostatic energy harvester manufactured with MEMS processes is are shown in Figure 1.2. Although it is easily manufactured with these type of processes, it needs external voltage sources or electrets. This situation restricts it's practical use and . In addition to this, since there is parasitic capacitances in the structure, the efficiency of the generator decrease.

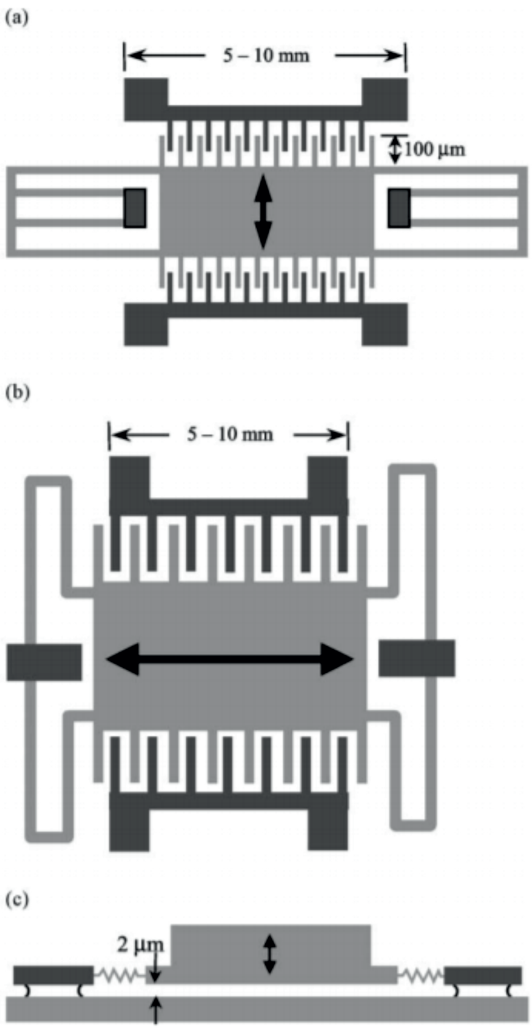

Figure 1.2. Three Different Type of Electrostatic Energy Harvester. [8]

Piezoelectric generators are based on molecular properties of piezoelectric materials. These materials has negative and positive charges balanced around a molecular gravity centers under no load [9]. When a load applied on the piezoelectric materials, the molecular balance disturbed and dipoles are occurred. These dipoles polarize the piezoelectric substance. In order to cancel out this unbalanced dipoles, there will be charge flow. The piezoelectric devices do not require a external voltage source as electrostatic devices. They also can be produced as micro and macro scale. The example of piezoelectric device model is shown in Figure 1.3. Piezoelectric energy harvesters are produced in abundance as a commercial product that converts mechanical energy into electrical energy because of its advantages over electrostatic and electromagnetic generators. However, this devices require some special materials such as PZT or ZnO. They also need to polarize in certain direction. This situation complicates the integration of these films in to circuits and makes them fragile [3].

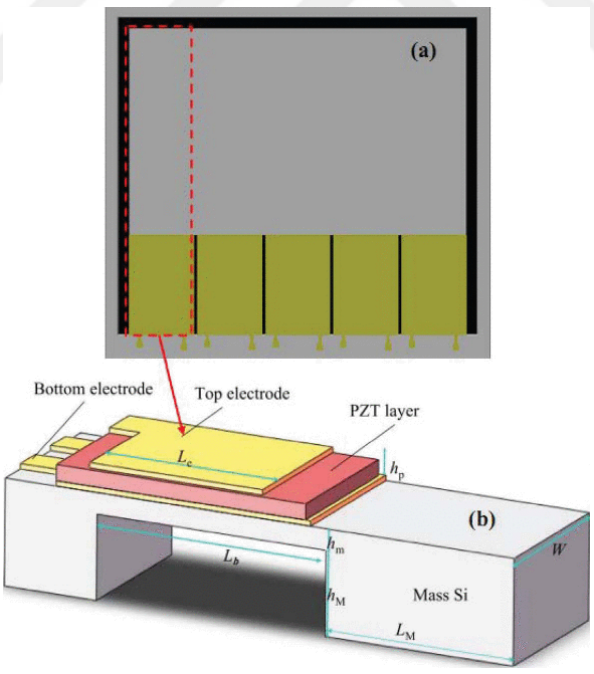

Figure 1.3. The Example of Piezoelectric Generator Model [10].

Although electromagnetic, electrostatic and piezoelectric energy harvesters are produced in order to convert mechanical energy to electrical energy, all of them has several disadvantages. Because of this, triboelectric energy harvesters are becoming popular in recent years [11]. The contact and separation of the two different surfaces which are generally polymer, cause a opposite but fixed charges on these two surfaces [12]. These charges can be collected by electrostatic induction through the electrodes on the back of the solid surfaces. This effect offers prospect in energy harvesting in recent years [13]. Since, it is worked with only surface effect, the overall system can be light weight and flexible. Because of it is processed with cheap thin films like polymer it can be produced at a low-cost and it can be spread in wide areas. The amount of energy produced can be increased by stacking layers on top of each others. It is simple to develop and produce. It is sufficient to use two materials which can be positively and negatively charged in contact and to form electrodes on their back surfaces [14].

1.1. Triboelectric Effect

The triboelectric effect, also called triboelectrification effect is a contact electrification in which two different materials get a contact and because of the friction these materials become electrically charged with opposite charges. This effect can be seen as electrostatic in people's daily life because of the a people's movement, wind, animals or any movement caused friction. According to materials relative polarity materials keep a different signed charges.

The triboelectric effect is known since almost start of the human existence. It is generally taken under consideration as undesired effect. Electrostatic discharge is a result of this effect and it can cause minor discomfort to the humans, critical damage to electronic equipment and even fires and explosions if the air contains combustible gases or particles. Even very small portion of this effect can cause the integrated circuits to become completely unusable due to high voltage. Hence, electronic devices, transportation vehicles especially planes, chemical industrial products has a protection protocol for this effect beginning from the manufacturing stages to consumer.

The triboelectric effect is started to used as generator last centuries. Wimshurst machine and Van de Graaff generator are the popular examples [15]. This traditional machines are used as a high voltage sources which are collect charges came from triboelectric effect, and cause a high voltage. In these machines there is no current flow, however when the accumulated charges reach a certain level the charge is discharging by corana discharge. These two machines and the discharging mechanism is shown in Figure 1.4.

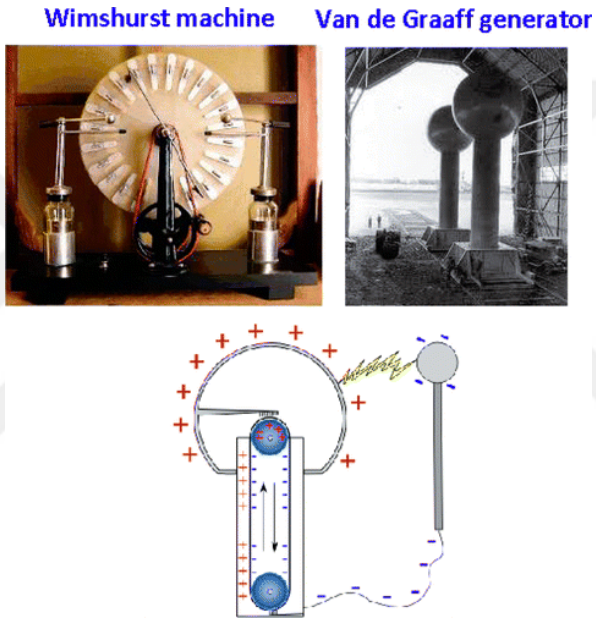

Figure 1.4. Wimshurst Machine and the Van de Graaff Generator with their discharge mechanism [15].

Although triboelectric effect has a long history, it's fundamental knowledge is still debated. According to the generally accepted view, when two different surface in contact there is a charge movement between these two surfaces. After separation some materials tend to hold this charges while others has a opposite tendency. Measurements were made in many different laboratories to compare these trends of materials [16]. The triboelectric affinity series is shown in Figure 1.5. In the last years according to this triboelectric series triboelectric nano generators has started to be developed. These new devices appears to have the potential to have a large share of the energy harvester which convert to mechanical energy to electrical energy.

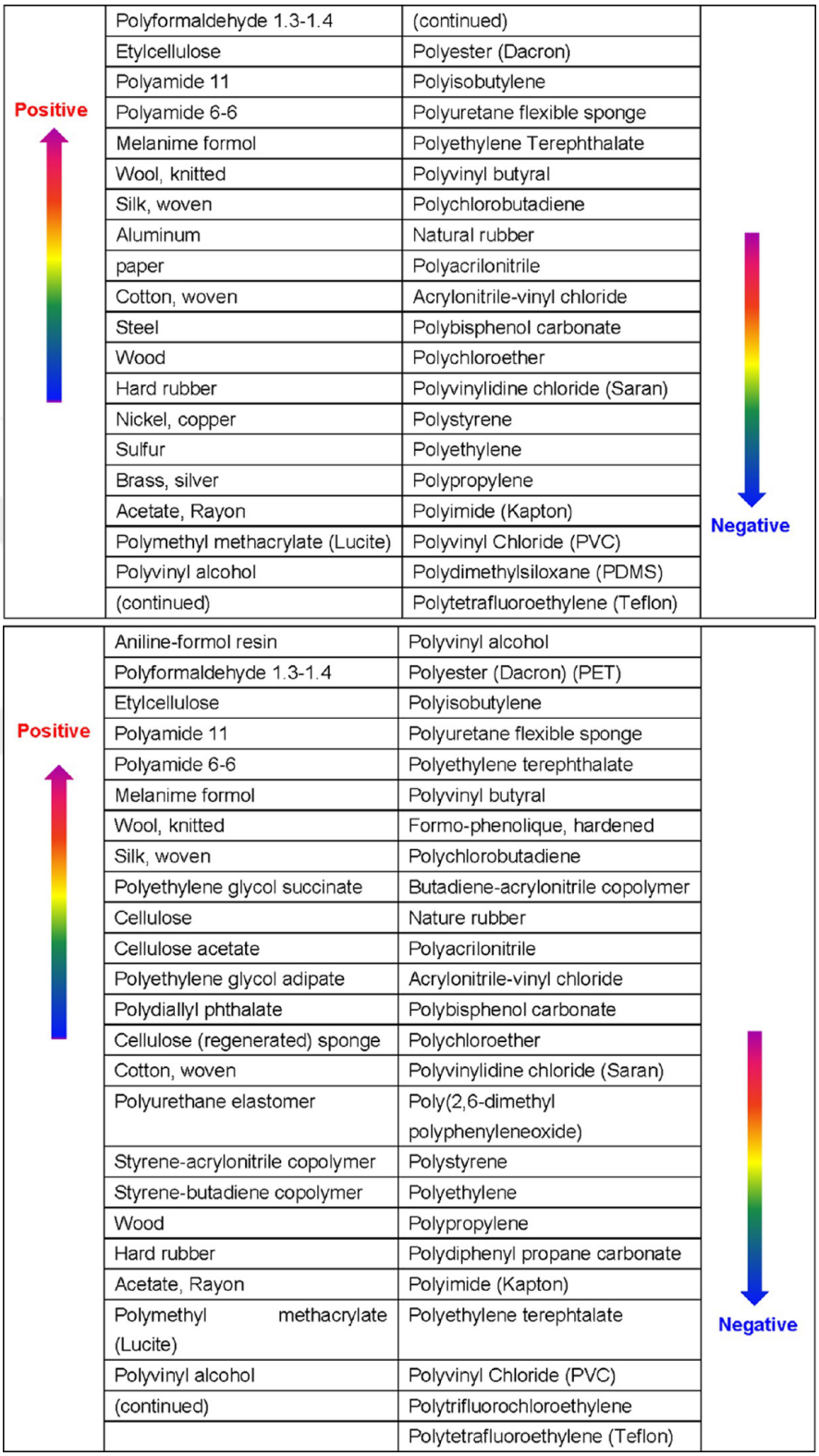

Figure 1.5. Triboelectric series [15, 17].

1.2. Motivation and Novelty

In today's world, the use of electronic devices has been varied. In addition to the commonly used power hungry devices, more and more low power devices, such as MEMS sensors and actuators, are introduced to the market. Triboelectric nano generators seem to be able to meet the energy requirements of these low power devices even though they can not reach the power levels of the power hungry devices. Hence, combination of energy harvesters with low power devices can be very beneficial. The integration of TENG's, which are easy and cost-free to produce in every dimension, with these low power devices can meet the needs in this area and cause much more useful products to emerge.

The purpose of study is to produce TENGs that can be used with higher efficiency by using different methods and show that these TENGs are useful for low power products by using these TENGs to provide the energy of simple IoT applications. Low power RF communication with bluetooth is used as IoT application.

Since the energy produced in the triboelectric energy harvesting method is directly proportional to the surface area, the nano structured polymer surfaces are produced and the generated energy is increased [15]. In order to produce nano structured polymer surfaces, formation of micro structures by lithography and soft lithography, roughing of surfaces with oxygen plasma at nano level, enlargement of nano tubes and nano wires by CVD and other alternative methods on the surfaces methods are used in several research [15]. However, there is no research that attempt to produce nano structured surfaces by synthesizing polymer brushes on polymer surfaces. The development of polymer nano structered surfaces with polymer brushes for triboelectric harvesters is novel.

In addition, steel and polymer surfaces have not yet been used in triboelectric energy harvesters using MEMS structures, although steel is shown among the most positively chargeable materials on the triboelectric series list. Because of the Young Modulus of the steel is slightly higher than silicon, it is mechanically as good as at least

silicon. Since the density of steel is 3.3 times that of silicon and it is not as brittle as silicon, even very thin steel films can be held by hand and passed through production stages. Taking advantage of this situation, moving mechanical structures produced by electrochemical etching from thin steel films integrated with polymer micro structures are fabricated [18–20]. Triboelectric harvesters which contain micro fabrication of steel films have not been shown before, which is a novel aspect of this study.

1.3. Outline of the Thesis

Up to this points in Chapter 1 methods used to meet the energy needs of electronic devices are mentioned. Following this some energy harvesters are introduced with their advantages and disadvantages. Then triboelectric harvesters and the mechanic behind them is briefly presented. Finally, the motivation and the novelty of this study are told.

In Chapter 2, different structures of the triboelectric nano generators are mentioned. Then, the physical mechanism behind this devices are described. Lastly, the mathematical model of TENG was derived.

In Chapter 3, the fabrication step of the three different harvester are described and explained in detail.

In Chapter 4, the instruments used during measurements are introduced. Then the measurement and characterization results of the each harvester are presented. Also, the applications with the generators are described and the results of the applications are showed.

In Chapter 5, a summary of the results is given briefly. Then this thesis is concluded with the future works can be done.

2. THEORY

2.1. Triboelectric Nano Generator

TENGs are energy generators that can be used to turn mechanical movements into electrical energy. There is different type of structures for triboelectric energy harvesting. Sliding mode and contact mode are frequently used structures. The sliding mode TENGs consists of two surfaces designed to slide on each other. As these surfaces rub on each other, the friction between these two surfaces results in a charge exchange. This exchange allows to the surfaces to be charged at the opposite signs, depending on the material's location in the triboelectric series. In this structure, there is also two electrode on the backside of the surface material. Sliding movement also change the capacitance between these electrodes. Hence, when there is a load between these electrodes, energy generated by electrostatic induction and triboelectric effect can be transferred to the load.

Contact mode TENGs are also consists two surfaces with the electrodes their backsides. These surfaces are positioned facing each other with a gap, that can be changed by applying mechanical force, between them. The surfaces of the contact mode TENGs can be both dielectric material as well as only one of them has a dielectric material and the other one is conductor. If the one of the surfaces is conductor, this surface serves both as a triboelectric layer and as an electrode. When the gap between the two surfaces of the TENG is closed by applying an external force, a frictional contact occurs between the two triboelectric surfaces. During this contact, the charge exchange occurs due to the triboelectric effect between the two surfaces. So the two surfaces are charged with opposite signs. If it desired that the amount of the charge is high, then surfaces must be chosen as one of them is one of the most negative material in the triboelectric series and the other is the one of the most positive material. When the surfaces are separated from each other, there is a potential difference between the two surfaces. If a load is connected between the two electrodes, the energy resulting from this potential difference can be transferred to the load.

Contact mode TENG can easily harvest energy from daily motions, such as pressing, pushing, walking or tapping [21]. Since, this works aims to use lost energy during the daily motions, it focuses on the contact mode TENGs.

2.2. Mathematical Modeling

In this study, energy is generated by the contact mode TENG and this energy is transferred to a connected load. Some parameters need to be predicted in order to produce TENG in the most efficient way [22]. Therefore, TENG is modeled mathematically and simulations are made on this model. This mathematical model predicts the amount of voltage generated, the size of the gap to be left between the two surfaces to achieve the required values, and the amount of load that must be connected to achieve maximum energy transfer. The TENG to be produced is designed as a conductor-to-dielectric type. The TENG produced in this way can be modeled as a variable voltage source and a series connected variable capacitance. This model is illustrated in Figure 2.1. The x(t) is the gap between two triboelectric layer and d is the thickness of the dielectric material which is used as polymer. In the mathematical model some parameters, which are ϵ_0 as a dielectric constant of air, ϵ_r as a dielectric constant of the polymer and σ as a surface charge density which is the density of the charge formed due to the triboelectric effect, are also used.

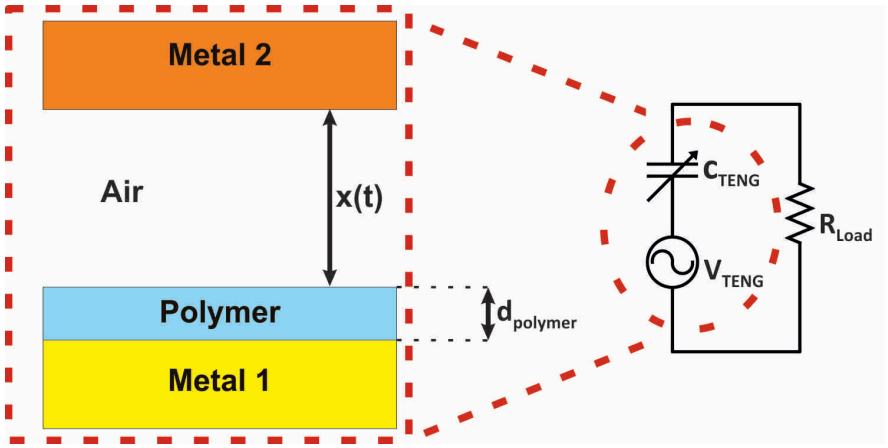

Figure 2.1. TENG model.

In the model voltage difference between triboelectric layers are defined as V_{TENG} and the charges formed on the electrodes because of this voltage is defined as Q. Since the surface area size (A) is the much larger than the distance between electrodes which is x(t)+d, charges on the electrodes can be assumed as evenly distributed. Hence the electric field between these electrodes is perpendicular to the surface. Then the electric field in the polymer can be given as

$$E_p = -\frac{Q}{A\epsilon_0\epsilon_r} \tag{2.1}$$

and in the air is

$$E_{air} = \frac{-\frac{Q}{A} + \sigma}{\epsilon_0}. \tag{2.2}$$

The voltage difference between electrodes is showed in Eq. 2.3.

$$V_{TENG} = E_p d + E_{air} x(t) \tag{2.3}$$

Eq. 2.3 can be rewritten as Eq. 2.4 by placing the Eq. 2.1 and Eq. 2.2 in the Eq. 2.3.

$$V_{TENG} = -\frac{Q}{A\epsilon_0}(\frac{d}{\epsilon_r} + x(t)) + \frac{\sigma x(t)}{\epsilon_0} \tag{2.4}$$

From the Eq. 2.4 the values which are important for the simulation model can be derived. One of them is the open circuit voltage. Since there is no charge transferred in the open circuit, Q=0. Hence the open circuit voltage can be written as Eq. 2.5.

$$V_{OC} = \frac{\sigma x(t)}{\epsilon_0} \tag{2.5}$$

The other important variable is C_{TENG}. The charges cause the open circuit voltage is trapped in the polymer surface. Hence, these charges do not flow over the capacitance. If these charges are omitted the voltage difference over the capacitance can be expressed as Eq. 2.6.

$$V_C = -\frac{Q}{A\epsilon_0}(\frac{d}{\epsilon_r} + x(t)) \tag{2.6}$$

The C_{TENG} can be estimated by combining Eq. 2.6 with the simple correlation, between voltage and capacitance, shown in Eq. 2.7.

$$C = \frac{Q}{V} \tag{2.7}$$

The C_{TENG} can be derived as in Eq. 2.8 by the combination of Eq. 2.6 and Eq. 2.7.

$$C_{TENG} = \frac{A\epsilon_0}{\frac{d}{\epsilon_r} + x(t)} \tag{2.8}$$

3. FABRICATION

Three different TENG structure fabricated in this study. First one has the polymer surface in one of the triboelectric layer and the steel electrode on the other layer. It has 1 cm^2 effective surface area. As a polymer, in addition to polydimethylsiloxane (PDMS), polymer nano structured surfaces with polymer brushes are used. Polystyrene (PS) and poly(pentafluorostyrene) (PPFS) are used as polymer brushes. Second TENG is manufactured in macro scale. This one has the Polytetrafluoroethylene (PTFE) as one of the layer and steel electrode on the other layer. PTFE and steel were also used as triboelectric layers for production of the last TENG. However, the steel electrode, in this TENG, is microfabricated first. Steel layer has crab leg shape and it also has 1 cm^2 effective surface area.

3.1. Fabrication of TENG with Nano Structured Polymer Surfaces

The first step of the fabrication is preparing PDMS surfaces with aluminum electrode at backside. For this process, Sylgard 184 silicon elastomer is used. The elastomer is contained in a clean bottle in a curing agent:elastomer ratio of 1 to 3. Then it is mixed with a rod for 5 minutes. At the same time, aluminum electrode is kept under the oxygen plasma for 1 minute in order to activate it's surface. In this way better adhesion of PDMS is achieved. The prepared polymer is coated on aluminum surface. The PDMS thickness is set to be approximately 150 μm. After this step, the sample left to dry for 24 hours. Processed PDMS-Al samples are cut into 1x2 cm size with scissors and taken into polymer brush process. It is planned to use 1 cm^2 of the samples as the triboelectric surface area while the remaining part is planned to be used as wire contact area.

The polymer brush is a polymer chain of which one end is attached to a surface. The dens presence of the polymer brush can provide roughness on the surface. Since it is predicted that this roughness may increase the charge density caused by the triboelectric effect, polymer brushes formed on PDMS surface. The formation

of the polymer brush was made by the chemistry department. In order to be able to form polymer nano brushes on the surface of PDMS, it's surface is chemically attached to radical initiators. Polymers are grown from these starting points. Because of the hydroxyl groups (-OH) on the PDMS surface, only poly (methyl methacrylate) (PMMA) or polystyrene (PS) nano brushes can be enlarged. Since PS is more negative in triboelectric series, PMMA is not used.

The PS nano brush growth steps on the PDMS surface are shown in Figure 3.1. In order to grow polystyrene over PDMS surfaces, they are first coated with the chain transfer agent required for polymerization. Clean PDMS surfaces were left in the solution of the Reversible Addition–Fragmentation Chain Transfer (RAFT) agent in dichloromethane for 24 hours. The remaining RAFT polymerization agents were then removed by washing with dichloromethane and methanol, after which the surfaces were dried under nitrogen gas. 75 mmol Styrene and 0.025 mmol polymerization initiator (AIBN) were taken up in a vessel containing magnetic stirrer and then dissolved in 5 mL toluene.Then nitrogen was passed through the solution for 20 minutes to remove oxygen from the atmosphere. The PDMS surface was then placed in a closed, oxygen-depleted vessel and the solution containing the styrene was transferred to the vessel. The polymer was grown on the surface at 80 °C for 18 hours. After 18 hours, remaining monomers are removed by washing to surface with toluene and acetone.

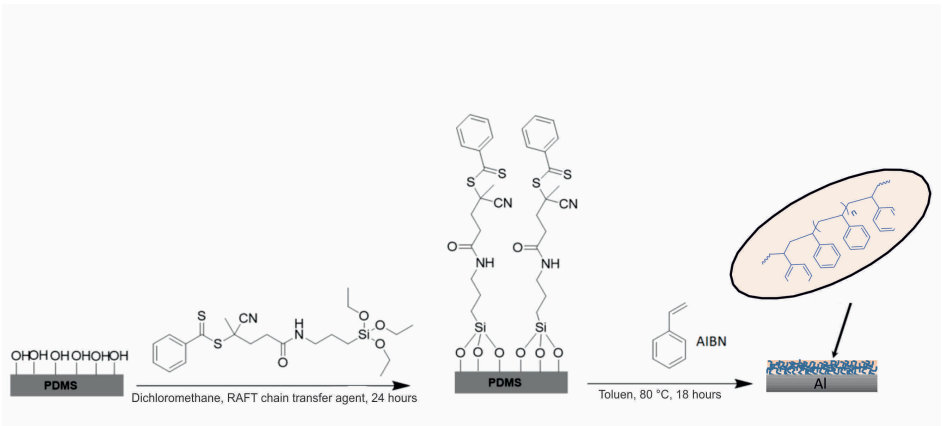

Figure 3.1. PS nano brush growth with chemical methods on PDMS surfaces.

When the triboelectric series are examined, it is seen that PDMS and polystyrene are close to each other in terms of negativity, whereas PTFE is seen as the material with the highest negativity. By taking inspiration from PTFE which has a structure containing fluorine; poly(pentafluorostyrene) (PPFS) nano brush, which is a chain containing fluorine is considered to be grown. PPFS has a similar structure to polystyrene. The PPFS growth on the surface of the PDMS is similar to the polystyrene. The only difference is using 37.5 mmol pentafluorostyrene and 0.0125 mmol polymerization initiator (AIBN) dissolved in 2.5 mL toluene instead of styrene solution. After the polymer was grown on the surface at 80 °C for 18 hours, the remaining monomers are removed by washing to surface with toluene and tetrahydrofuran (THF). The PPFS nano brush growth steps on the PDMS surface are shown in Figure 3.2.

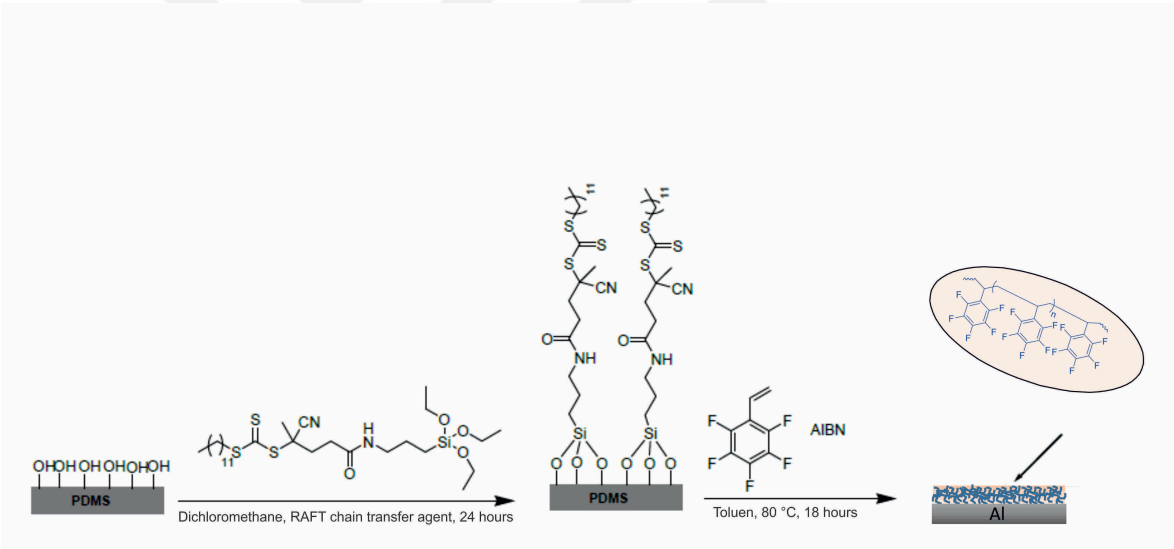

Figure 3.2. PPS nano brush growth with chemical methods on PDMS surfaces.

The presence of the polymer layer on the PDMS surfaces is primarily determined by X-ray photo electron spectrometry (XPS). When high resolution C 1s spectra of PDMS, polystyrene and poly(pentafluorostyrene) coated PDMS surfaces; it is seen that PS coated one has $\pi \rightarrow \pi^*$ transition peak resulting from aromatic group, and PPFS coated one has a peak because of C-F. General XPS spectra and high resolution scans of C 1s regions of PDMS, PS and PPFS coated PDMS is shown in Figure 3.3.

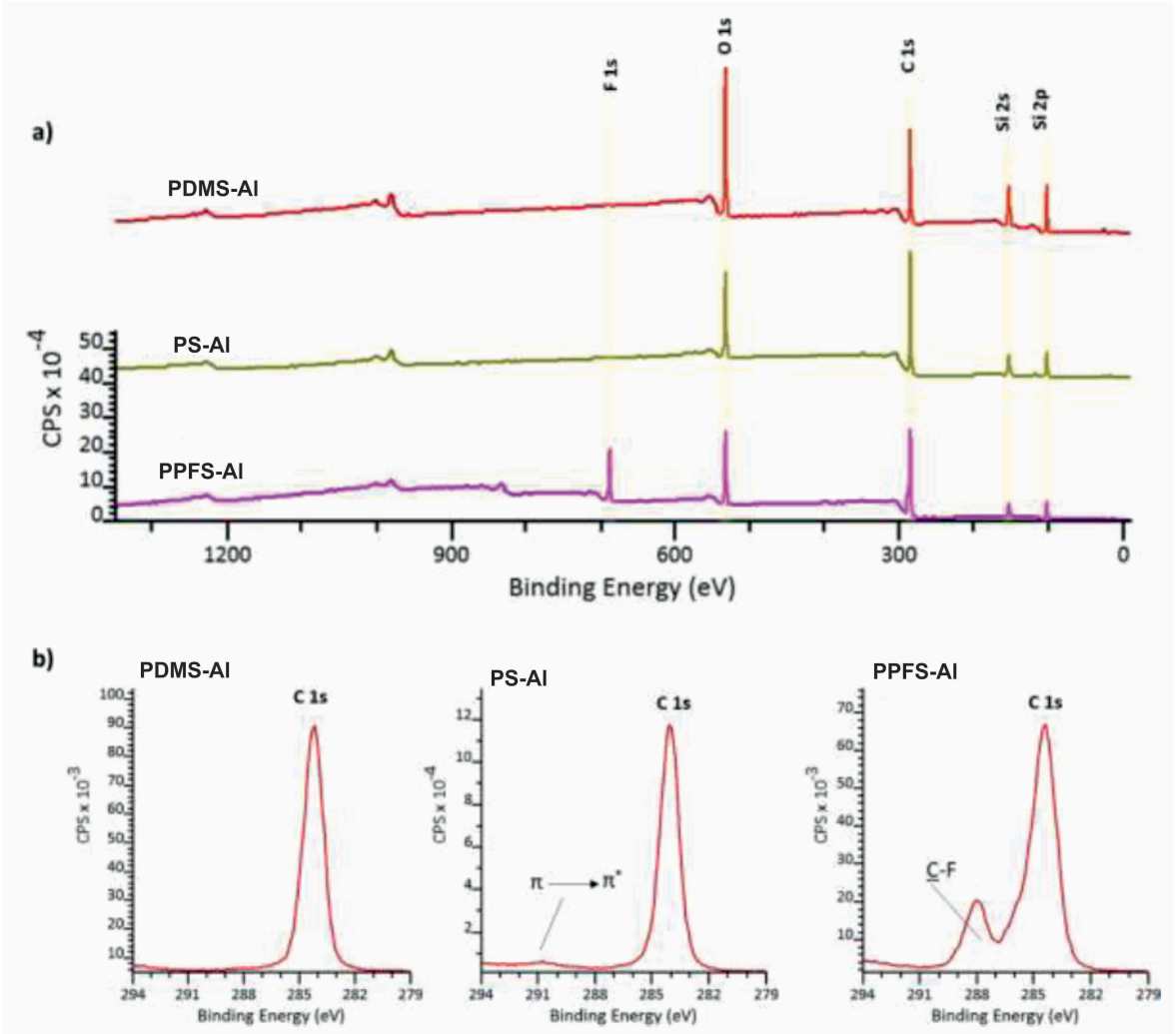

Figure 3.3. General XPS spectra of PDMS, polystyrene and poly (pentafluorostyrene) coated PDMS (a) and high-resolution scanning of C1s regions (b).

As a result of comparing the prepared surfaces with Fourier transform infrared spectroscopy (FTIR), the presence of polystyrene on the surfaces verified. In the FTIR results of PDMS with PS polymer brushes; in addition to asymmetric CH3 stretching in Si-CH3 at 2960 cm^{-1}, CH3 symmetric bending in Si-CH3 at 1257 cm^{-1} and Si-O-Si stretching at 1010 cm^{-1} and 1074 cm^{-1} which these are caused by PDMS; aromatic C-H stretching at 2800-3100 cm^{-1} and aromatic C=C stretching at 1450-1601 cm^{-1} were observed. These C-H and C=C stretchings are caused by polystyrene. Also, In the FTIR results of PDMS with PPFS polymer brushes, C = C aromatic stretching at 1498-1651 cm^{-1} and C-F stretching at 961 cm^{-1} and 980 cm^{-1} were observed. FTIR spectra of PS, PPFS coated PDMS surfaces and untreated PDMS surface is shown in Figure 3.4.

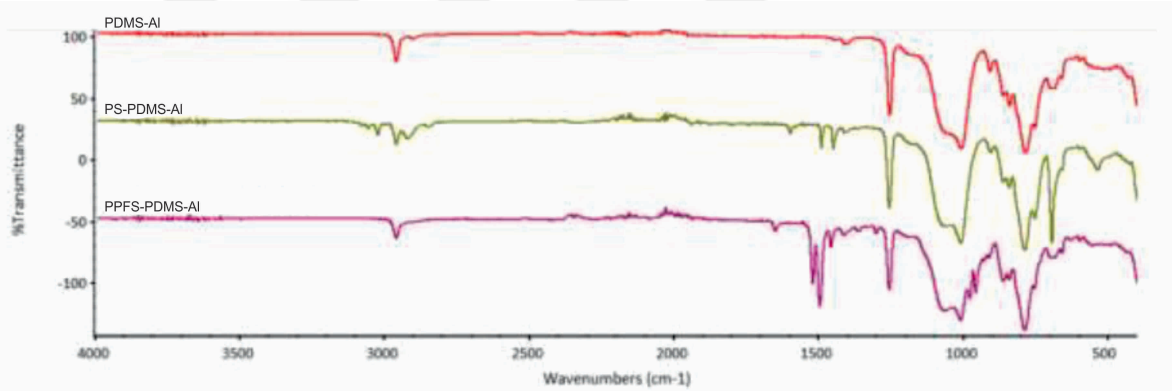

Figure 3.4. FTIR spectra of PS, PPFS coated PDMS surfaces and untreated PDMS surface.

As a last test the surface properties of polystyrene brush grown PDMS-Al is compared to the PDMS-Al coated with RAFT agent in toluene at 80 °C for 18 hours by zooming 5000 times with environmental scanning electron microscopy (ESEM). According to the images taken from the side sections of the surfaces, rough structure is detected on the surface has polymer brush while while the RAFT agent coated PDMS surface, which is left untreated in the polymerization conditions, has no roughness. The ESEM image of the samples is in Figure 3.5.

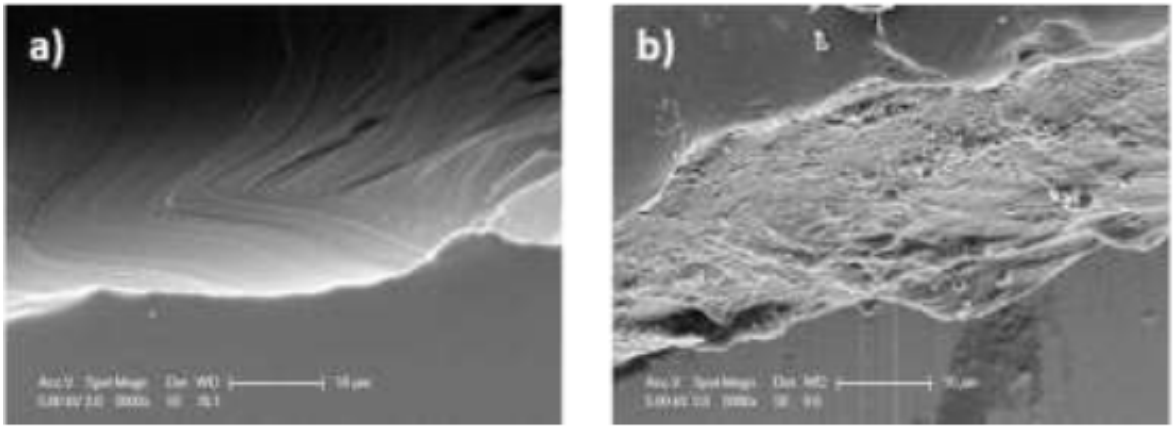

Figure 3.5. Comparison of ESEM images taken from the side sections of the surfaces. (a) RAFT agent coated PDMS-Al (5000x) (b) Polystyrene coated PDMS-Al (5000x).

It has been shown that polymer brushes are formed on the surface of the PDMS with xps, FTIR and ESEM results. Thus the production of the one of the triboelectric surface of TENG is completed. Untreated, PS coated and PPFS coated PDMS surfaces to be used as this layer is shown in 3.6.

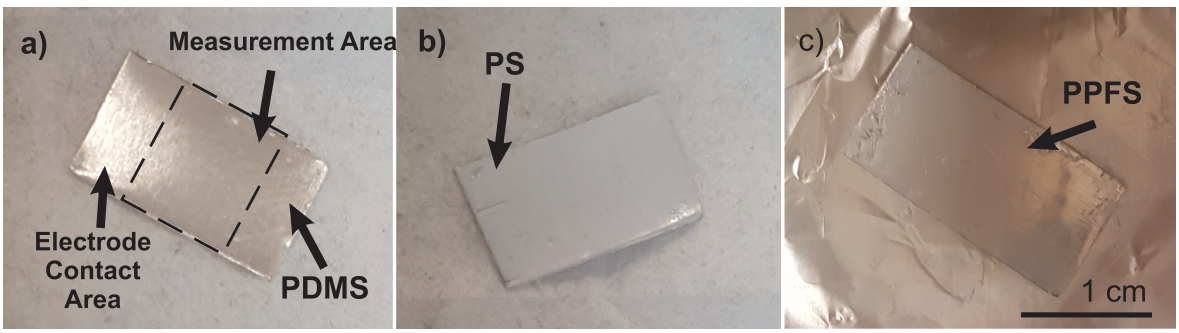

Figure 3.6. Untreated, PS coated and PPFS coated PDMS surfaces.

Later on, preparation of the TENG test setup was started so that measurements can be taken on these surfaces. Since surfaces are to be measured relative to each other, it is important that all experimental setups are identical. For this purpose, each sample is attached to a surface of a 3D printed block and mechanically tightly connected to a coaxial cable. This setup can be seen in Figure 3.7.

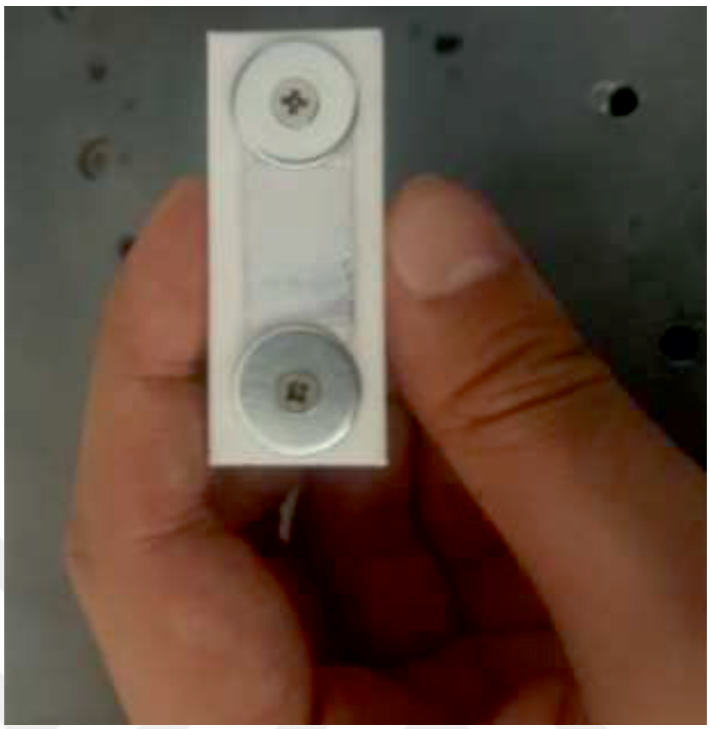

Figure 3.7. Nano structured surfaces placed on a test setup.

A steel electrode was used on the opposite surface of the nano structured surface. For this purpose, another 3-D printed block is prepared for the bottom surface. A flat steel electrode is then placed neatly on the surface of this block and tightly connected to a coaxial cable. The setup is shown in Figure 3.8.

Finally, the top surface is attached to a CNC head. Thus, the connection to the CNC machine, which provide the movement, was made. For repeatable pressing tests, the bottom and top surfaces are smoothly passed each other. With this structure, the effective surface area of TENG can be set to 1 cm^2. This structure also provide the same measuring environment condition for all surfaces produced. Completed TENG can be seen in Figure 3.9.

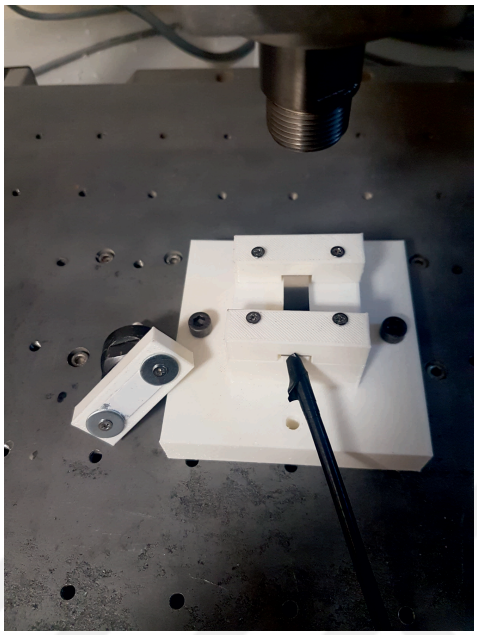

Figure 3.8. The setup for bottom and top surfaces.

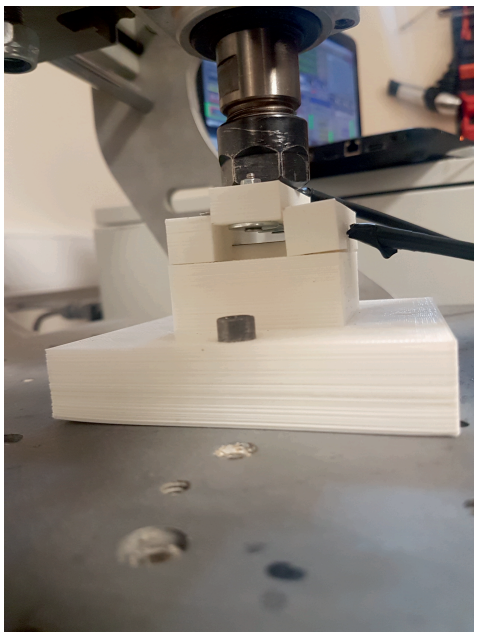

Figure 3.9. TENG with the nano structured polymer surface.

3.2. Fabrication of TENG with Microfabricated Steel Electrode

The first step is fabrication of the microfabricated steel electrode. Fabrication of this electrode consists of several steps such as lithography, electrochemical etching, wet etching, hot embossing and thermo-compression bonding. Detailed explanations of these steps are given in a previous study [21].

After these steps, the produced steel film was contacted with ultrasonic solder. Thus, the electrode is ready to be used as the top surface of the TENG. A block to be used as spacer for the movement of this electrode printed from 3D printer. A keyboard button like piece that is also printed from 3D printer is used for the movement to be in only z direction. Manufactured steel electrode and the button design can be seen in Figure 3.10.

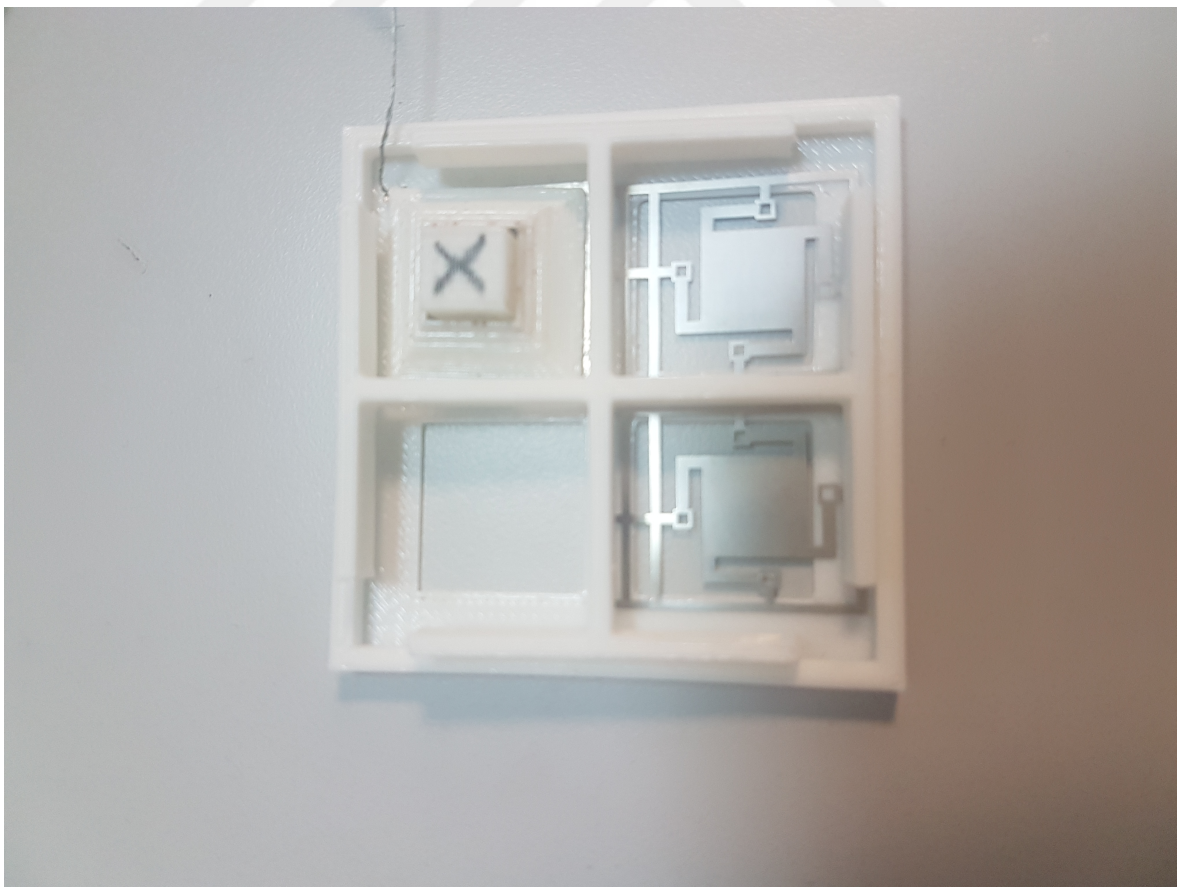

Figure 3.10. Keyboard button like design and crableg shaped steel electrode.

The PTFE surface with Al electrode is used as bottom layer of TENG. When this layer was prepared, 150 μm thick PTFE film was used. Then one side of this film is coated with 200 nm Al by using thermal evaporator. In thermal evaporation process, 0.5 gram Al is used and during the process the temperature at chamber is between 40°C and 60°C. This PTFE was then fixed on a flat surface and mechanically contacted to the Al plate behind it. The produced bottom layer of TENG is showed in Figure 3.11 and the complete TENG is in Figure 3.12.



Figure 3.11. Al coated PTFE film which is fixed and it's electrical contact is established.

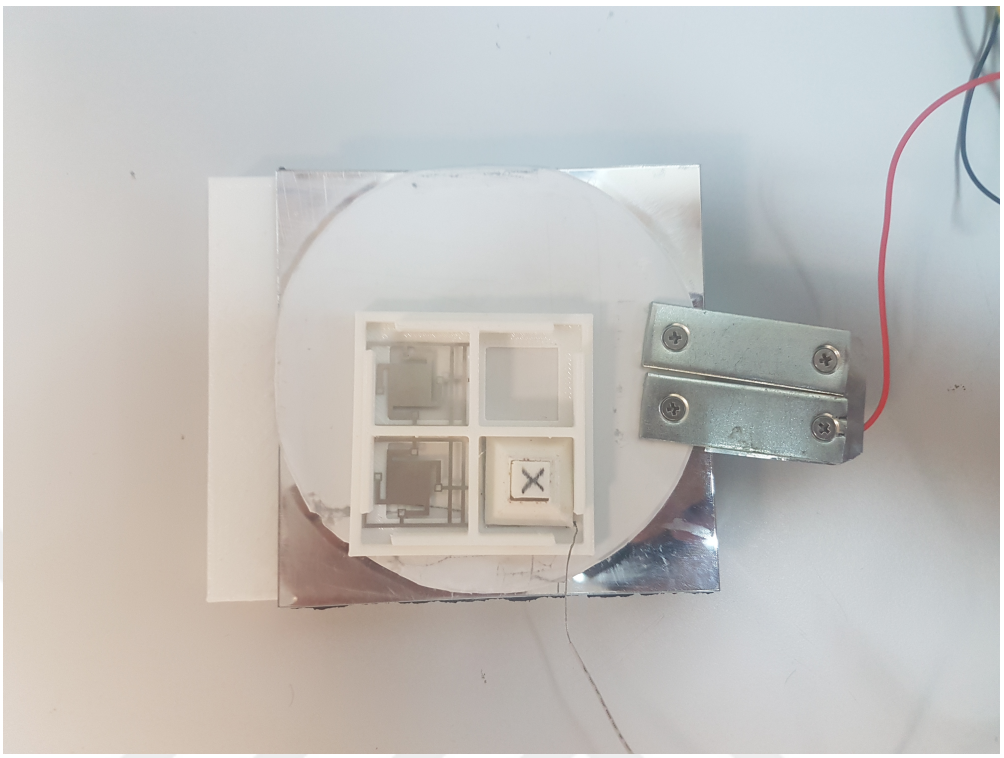

Figure 3.12. TENG with microfabricated steel electrode.

3.3. Fabrication of Macro Scale Triboelectric Generator

PTFE and steel is used as triboelectric surfaces for also macro scale generator. The first step of fabrication is printing a plastic block, which has 2 holes one within the other at every corner, from 3D printer. 4 springs are placed in the holes at corners. Steel rods are also placed in the gap of springs to provide stability during the movement. Then PTFE film is coated with Al as it is described in Section 3.2. Al coated PTFE film is fixed on plastic block and electrical contact with Al is established mechanically. Double sided tape is used in addition to mechanical compression for fixing. The effective area of PTFE is measured as approximately 60 cm^2. The bottom part of the generator is shown in Figure 3.13.

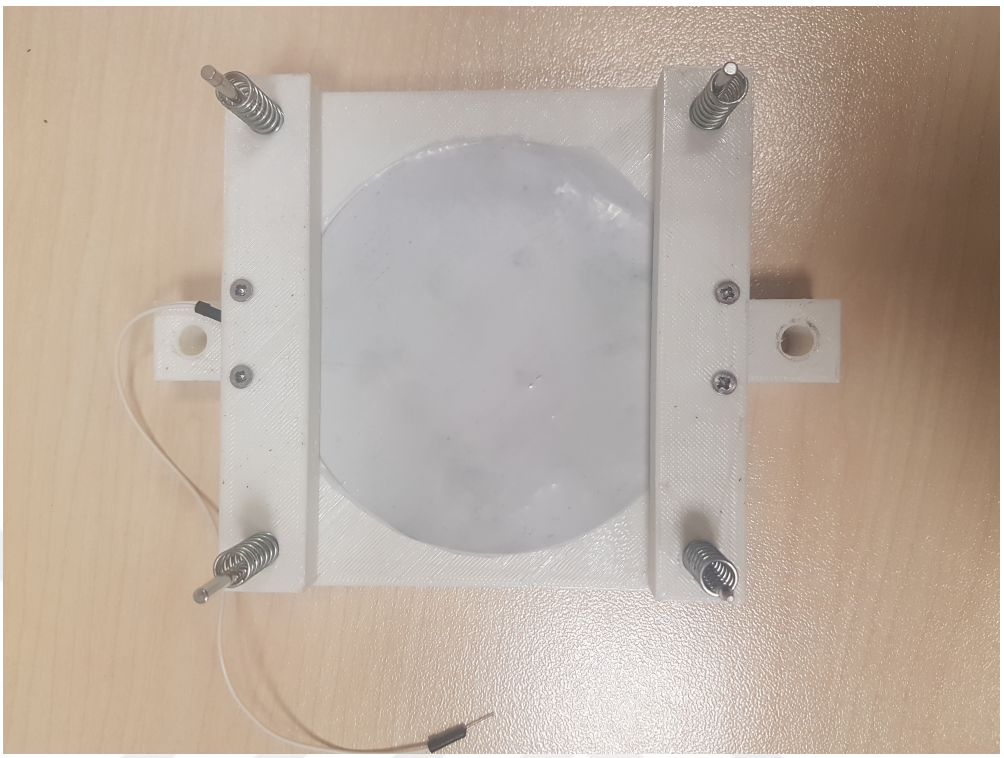

Figure 3.13. Bottom part of the macro scale triboelectric generator.

For the top part, another plastic block is printed from 3D printer. This block is designed as it is perfectly fit the bottom part. This block also has holes for springs and steel rods. After printing the block, 60 cm^2 steel film is cut by scissors as it is matched with the PTFE film in bottom part. When to parts are combined 1 cm of the springs remain outside. This remaining part provide a contact and separation movement when the force applied. The steel rods ensure this movement is in only z direction. The top part of the generator is given in Figure 3.14. The combined macro scale triboelectric generator is shown in Figure 3.15.

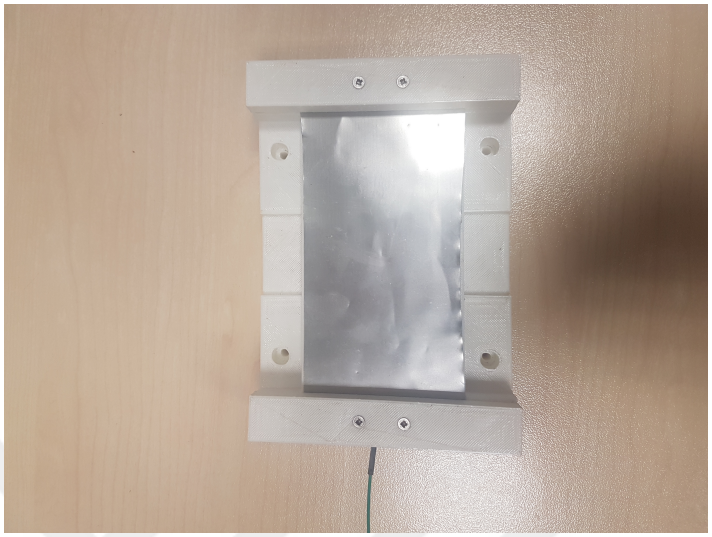

Figure 3.14. Top part of the macro scale triboelectric generator.

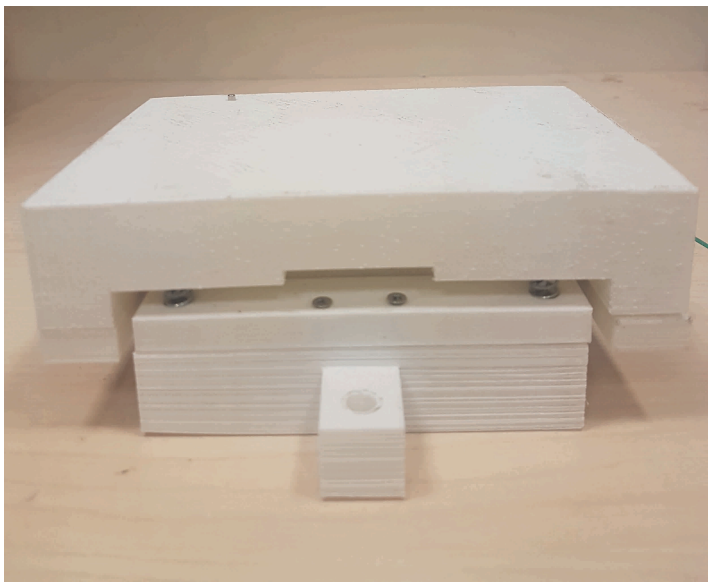

Figure 3.15. Macro scale triboelectric generator.

4. CHARACTERIZATION MEASUREMENTS AND RESULTS

4.1. Measurement Equipments

4.1.1. Electrometer

In this work, the current and voltage measurements are done with Keysight B2985A Electrometer/High Resistance Meter which can be seen in Figure 4.1. This device has the minimum 0.01 fA current, 1 μV voltage, 1 Ω resistance, and 1 fC charge resolution. Since the current value we take is so small for a basic oscilloscope; in order to get reliable measurement results, this device is used.



Figure 4.1. Keysight B2985A Electrometer/High Resistance Meter.

4.1.2. CNC Machine

TENGs produces energy by the action of contact separation. Therefore, it is vital that the z axis movement is performed in a stable manner so that a reliable measurement can be taken. CNC machine is used for this movement in z axis. The bottom surface of the measuring devices is fixed to the table of the CNC machine and the upper surface is attached to the CNC head with the aid of a 3D printer to provide a suitable environment for movement. The maximum gap between the triboelectric surfaces is also adjusted with the CNC machine. The CNC machine used in this study is shown in the Figure 4.2.

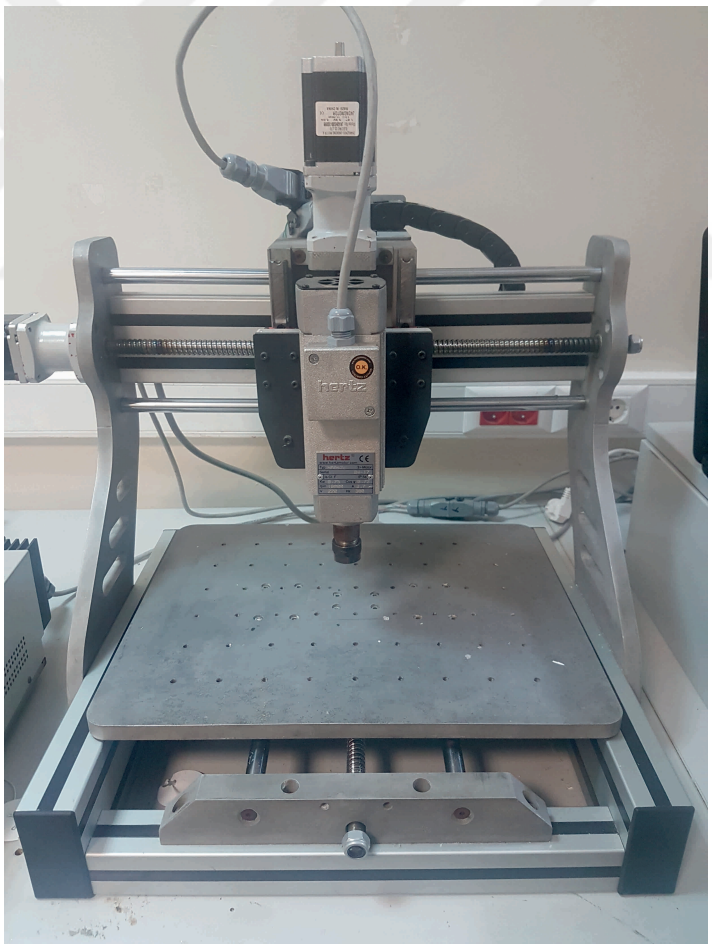

Figure 4.2. CNC machine.

4.1.3. Load Connection Setup

In order to find a maximum power transfer characterizations of the TENGs, they are measured with different loads. These loads were connected via a separate setup. In order to reduce to noise level in the system, this setup is connected to electrometer with triaxial cable and to TENG with coaxial cable. The connections in this setup are done with solder. The system is designed so that the desired resistance value can be easily inserted and removed. This setup can be seen in Figure 4.3.

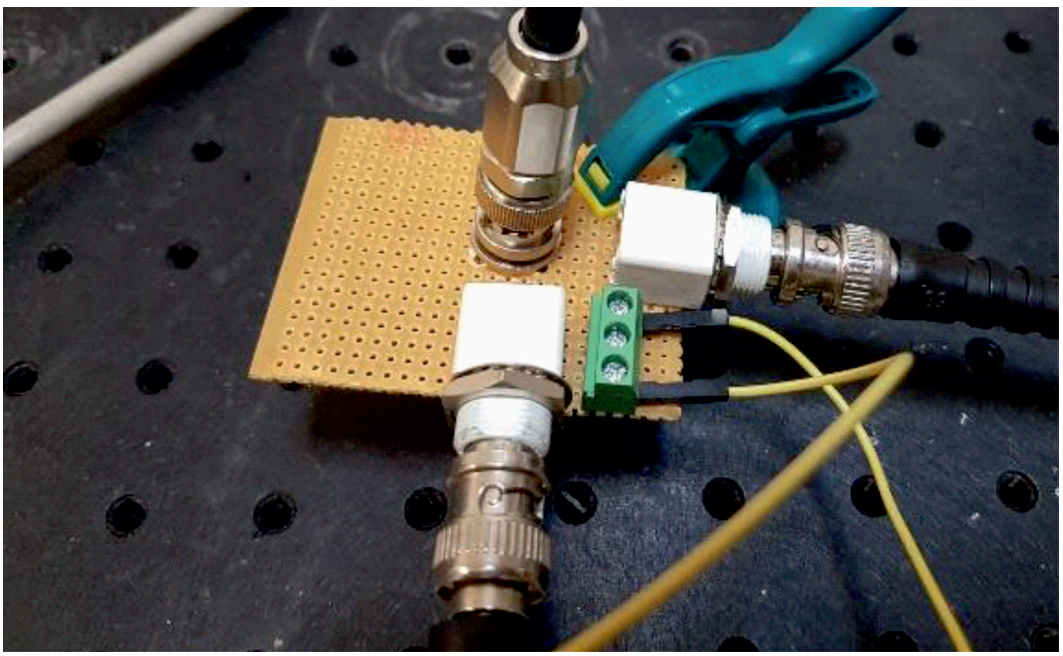

Figure 4.3. Load connection setup.

4.2. Measurements of TENG with Nano Structured Polymer Surfaces

PDMS, PS and PPFS measurements were made separately and then the results are compared. The effective area of each is set to be 1 cm^2. The gap between triboelectric layer is adjusted as 1 mm. During the measurements, the frequency of TENG's contact separation movement is approximately 1.5 Hz and it's velocity is fixed. Measurements were made using electrometer as current measurement and then transmitted power according to connected load value was calculated.

4.2.1. PDMS Measurement

PDMS measurements were made with load values ranging from 10 MΩ to 3 GΩ. Maximum transferred power is 45.7 nW at 300 MΩ. The current measurement at this load is shown in Figure 4.4. The instantaneous transferred power for different loads can be seen in Figure 4.5.

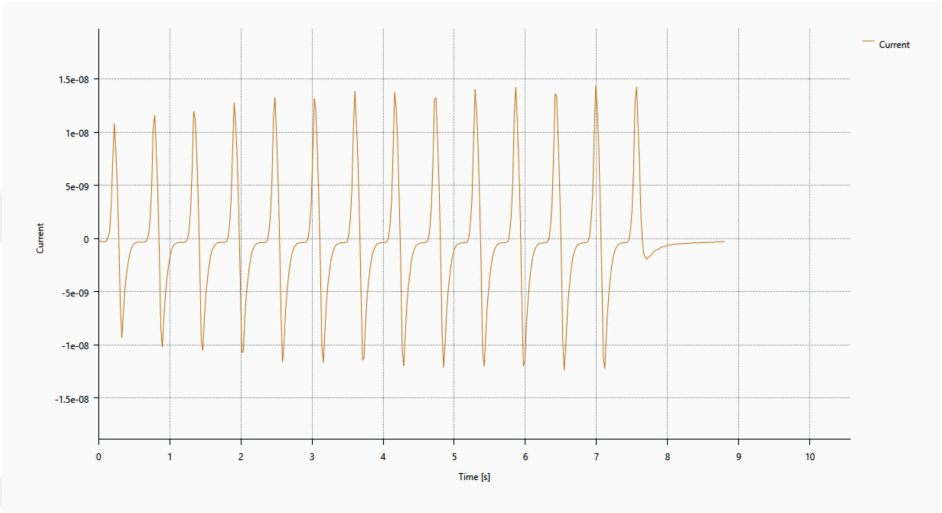

Figure 4.4. PDMS current measurement at 300 MΩ.

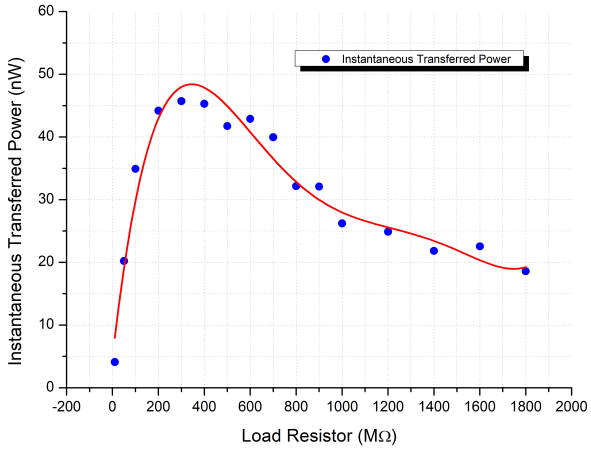

Figure 4.5. The instantaneous transferred power value for different load resistance for PDMS measurements.

4.2.2. Polystyrene Measurement

Since maximum power transfer is at 300 MΩ in PDMS measurements, it is assumed that the same behavior is observed for other polymers as well. Because of this, the highest load value to be measured is 1 GΩ in PS measurements. Maximum transferred power is 750.6 nW at 300 MΩ. The current measurement at 300 MΩ can be seen in Figure 4.6. The instantaneous transferred power for different loads is shown in Figure 4.7.

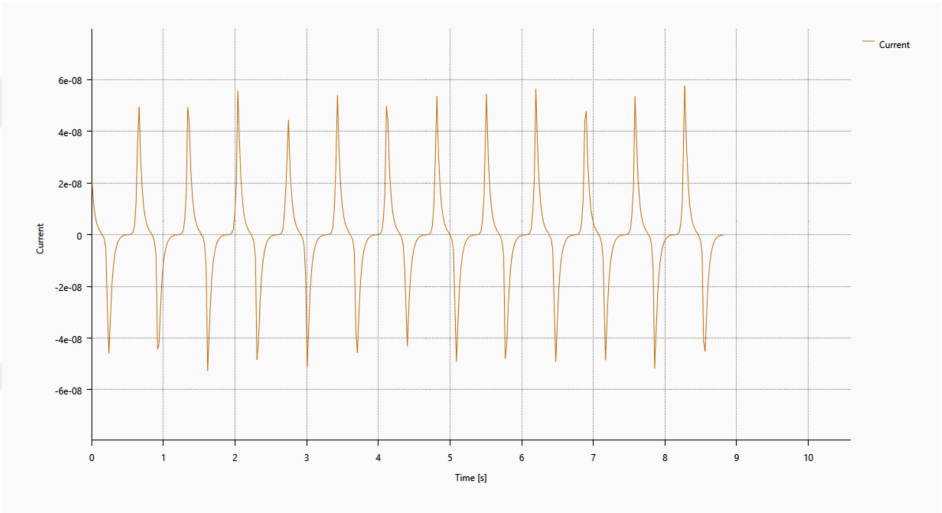

Figure 4.6. PS current measurement at 300 MΩ.

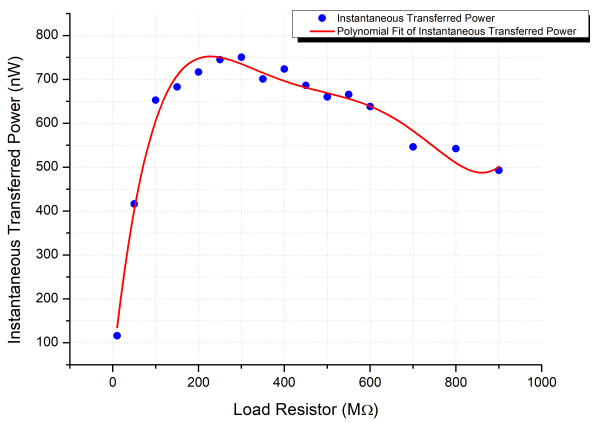

Figure 4.7. The instantaneous transferred power value for different load resistance for PS measurements.

4.2.3. Poly(pentafluorostyrene) Measurement

PPFS measurements were made with same load values used in PS measurements. In these measurements, the maximum transferred power is calculated as 2.3 μW at 250 MΩ. The current measurement at this load is shown in Figure 4.8. Although the maximum value is seen at 250 MΩ, there is no significant difference from the value at 300 MΩ. Therefore, it can be said that the results are consistent. The instantaneous transferred power for different loads for PPFS sample can be seen in Figure 4.9.

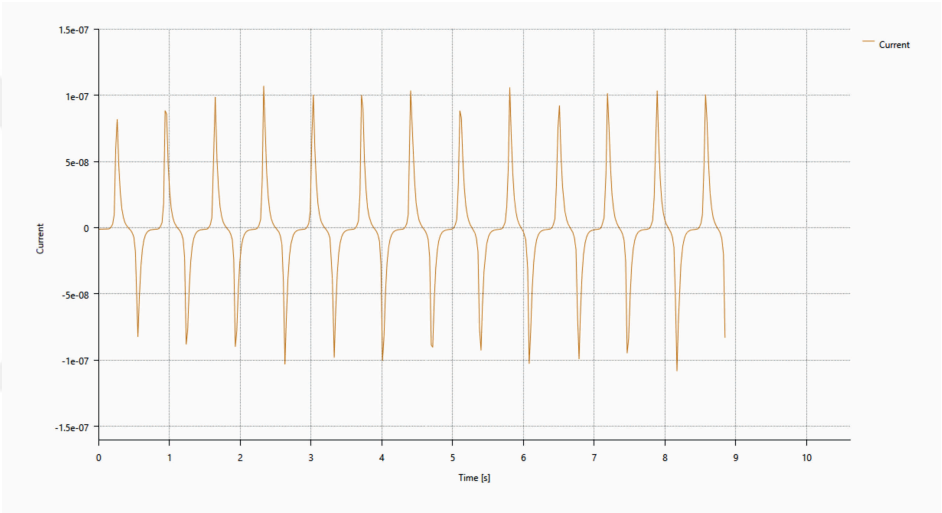

Figure 4.8. PPFS current measurement at 250 MΩ.

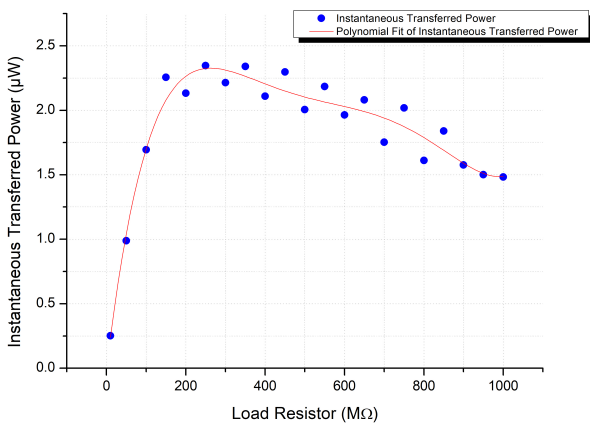

Figure 4.9. The instantaneous transferred power value for different load resistance for PPFS measurements.

4.2.4. Comparison of the PDMS, PS and PPFS Measurement Results

When the PDMS, PS and PPFS measurements are examined, the maximum power transfer is at close resistance value for all of them. It is clear that there will be maximum power transfer to load when the load resistance matched with the capacitance of the TENG (C_{TENG}). As it is seen in Eq. 2.8, (C_{TENG}) is proportional to surface area. Since the effective surface area for all this measurements is 1 cm^2, this results is suitable to theory.

There are significant differences when the power values produced are compared. While PS produces 16 times more power than untreated PDMS, PPFS generate 3 times more power than PS and 48 times more power than PDMS. These results show how effective the nano brush method is. Comparison of the current values of these three sample at 300 MΩ load resistor is shown in Figure 4.10 and transferred power comparison in Figure 4.11.

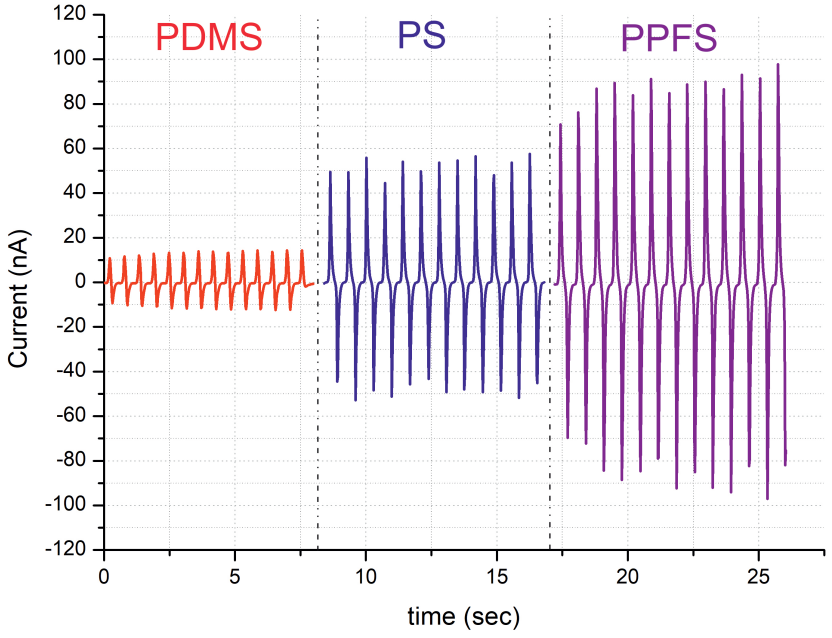

Figure 4.10. Current values of PDMS, PS, and PPFS at 300 MΩ.

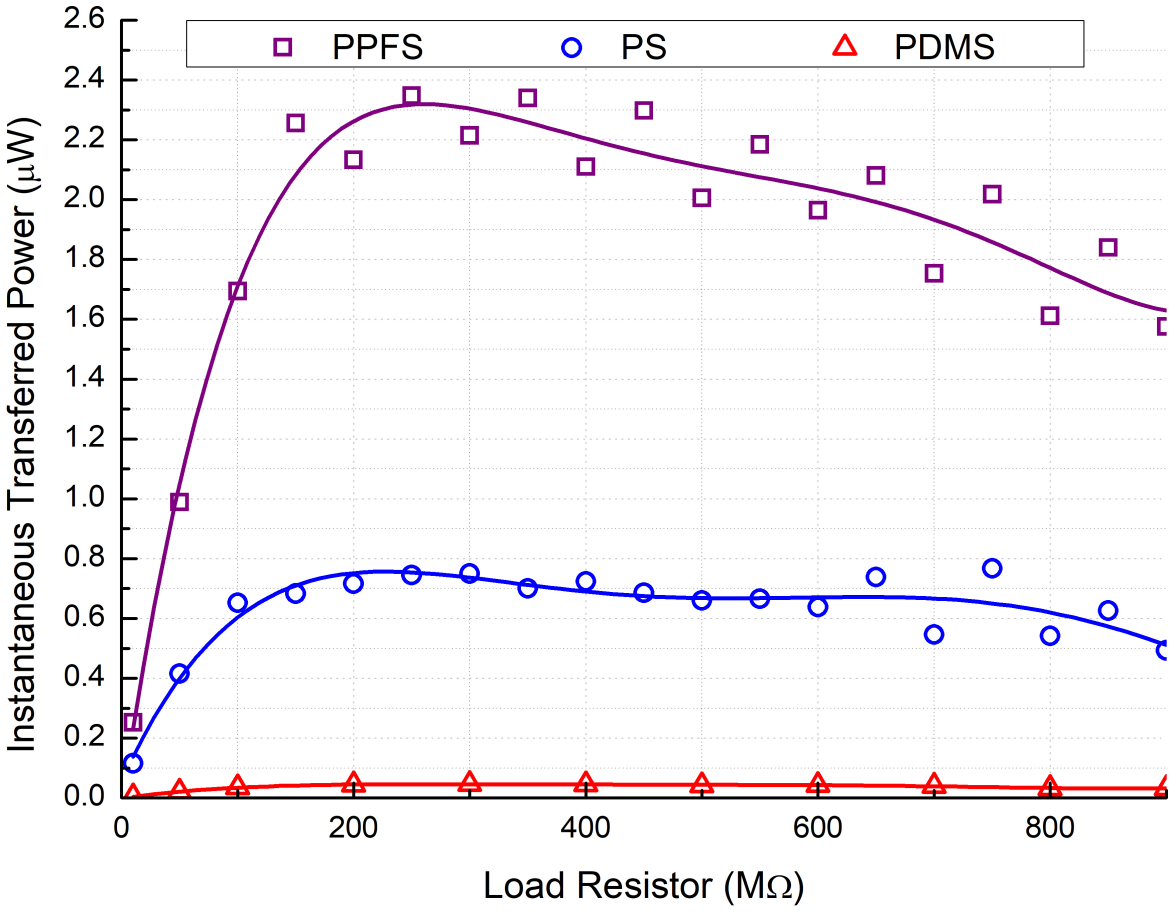

Figure 4.11. Transferred power values of PDMS, PS and PPFS for different load resistors.

4.2.5. LCD Application with Nano Structured TENG

Once the measurements have been completed, a simple LCD screen is displayed to visualize the harvested energy. Since PPFS has best power output characteristic between them, in application PPFS is used. In this application, nano structured TENG is connected to LCD via diode bridge rectifier. The on and off stages of the LCD display is showed in Figure 4.12.

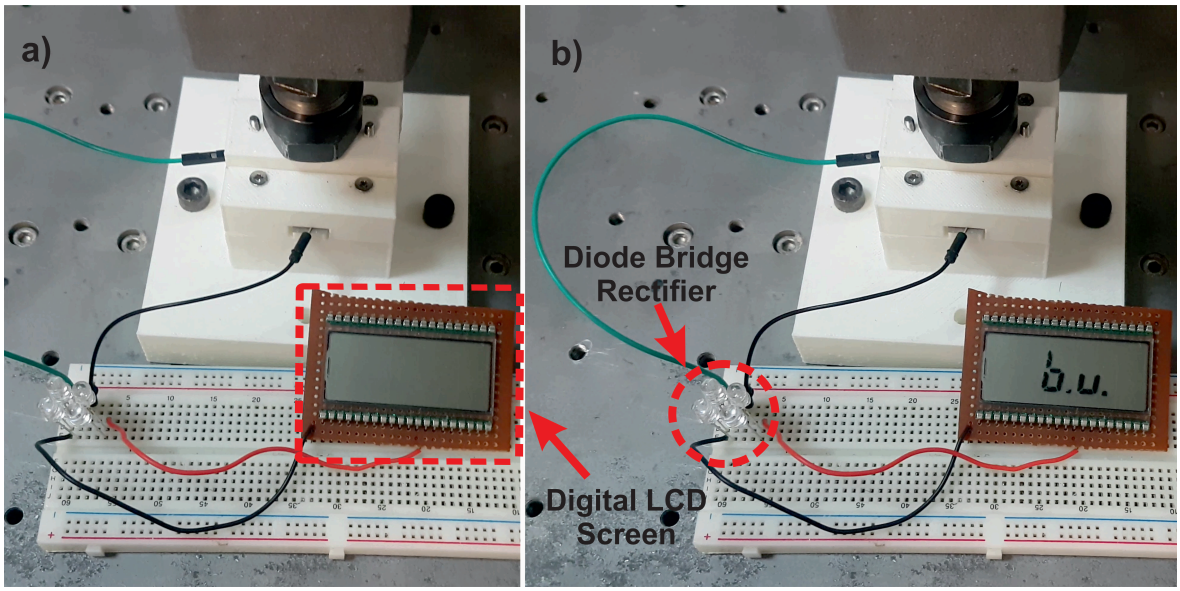

Figure 4.12. The LCD application setup. (a) TENG is at separation mode and (b) TENG is at contact mode.

4.3. Measurements of TENG with Microfabricated Steel Electrode

During the measurements of TENG with microfabricated steel electrode, as a load resistors range from 50 MΩ to 1 GΩ is used. In this measurements the movement force given by the hand instead of CNC machine. The gap between triboelectric layer is set to 1 mm. The maximum instantaneous transferred power is measured as 895 nW at 250 MΩ load. The current measurement at this load can be seen in Figure 4.13.

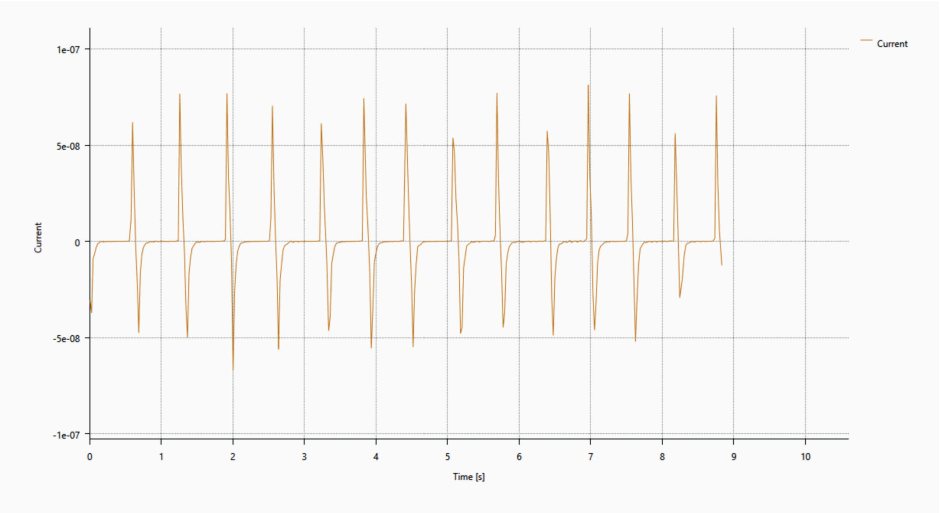

Figure 4.13. The current measurement of TENG with microfabricated steel electrode at 250 MΩ.

TENG with microfabricated steel electrode is also used in the LCD application. The TENG is directly connected to LCD this time. The results of the application can be seen in Figure 4.14.

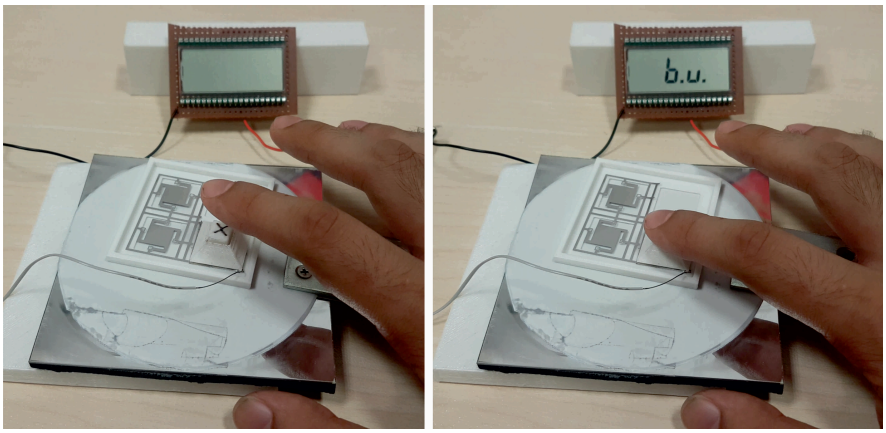

Figure 4.14. The LCD application setup of TENG with microfabricated steel electrode.

4.4. Measurements of Macro Scale Triboelectric Energy Harvester

During the measurement, the movement force is applied by CNC machine. The frequency of movement is set to approximately 0.75 Hz and the gap between triboelectric layer is 8 mm. The effective area of triboelectric area is 60 cm^2 as it is described in fabrication. The measured load resistors ranges from 10 MΩ to 250 MΩ. The maximum instantaneous power transfer is observed as 203 μW at 140 MΩ. The current measurement result in that value is shown in Figure 4.15 and the instantaneous transferred power value for different load resistances is in Figure 4.16.

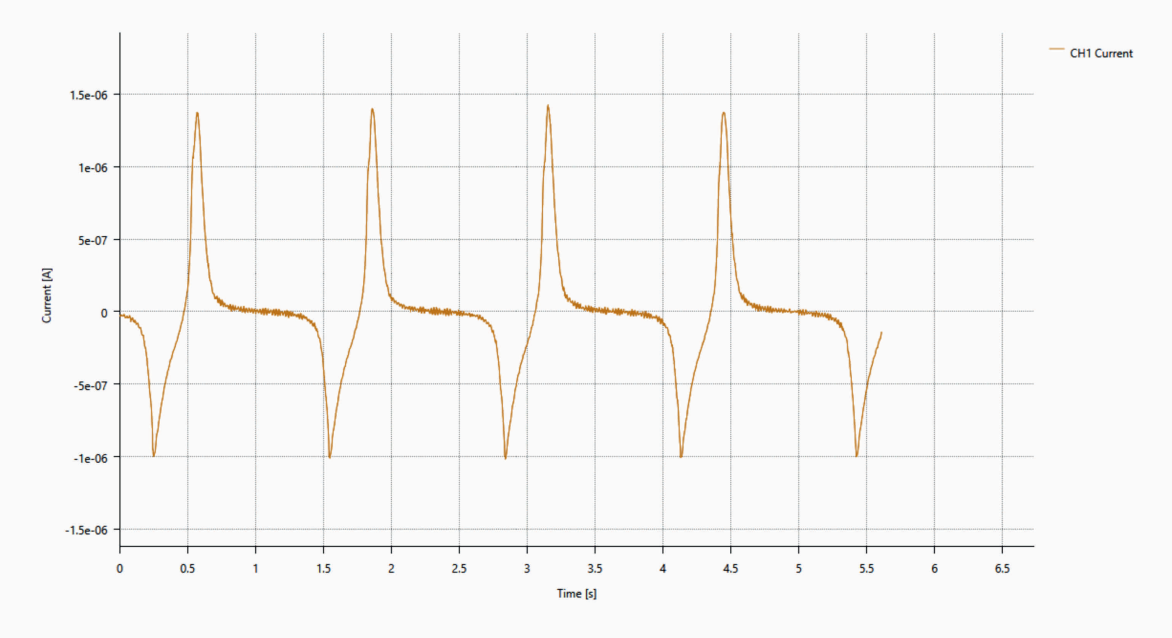

Figure 4.15. Macro scale triboelectric energy harvester current measurement at 140 MΩ.

With this device two different applications are planned. First one is the driving LEDs. For this purpose 196 commercial red LEDs is connecting each other serially. Then it is connected to triboelectric generator via rectifier bridge. The outcome is shown in Figure 4.17.

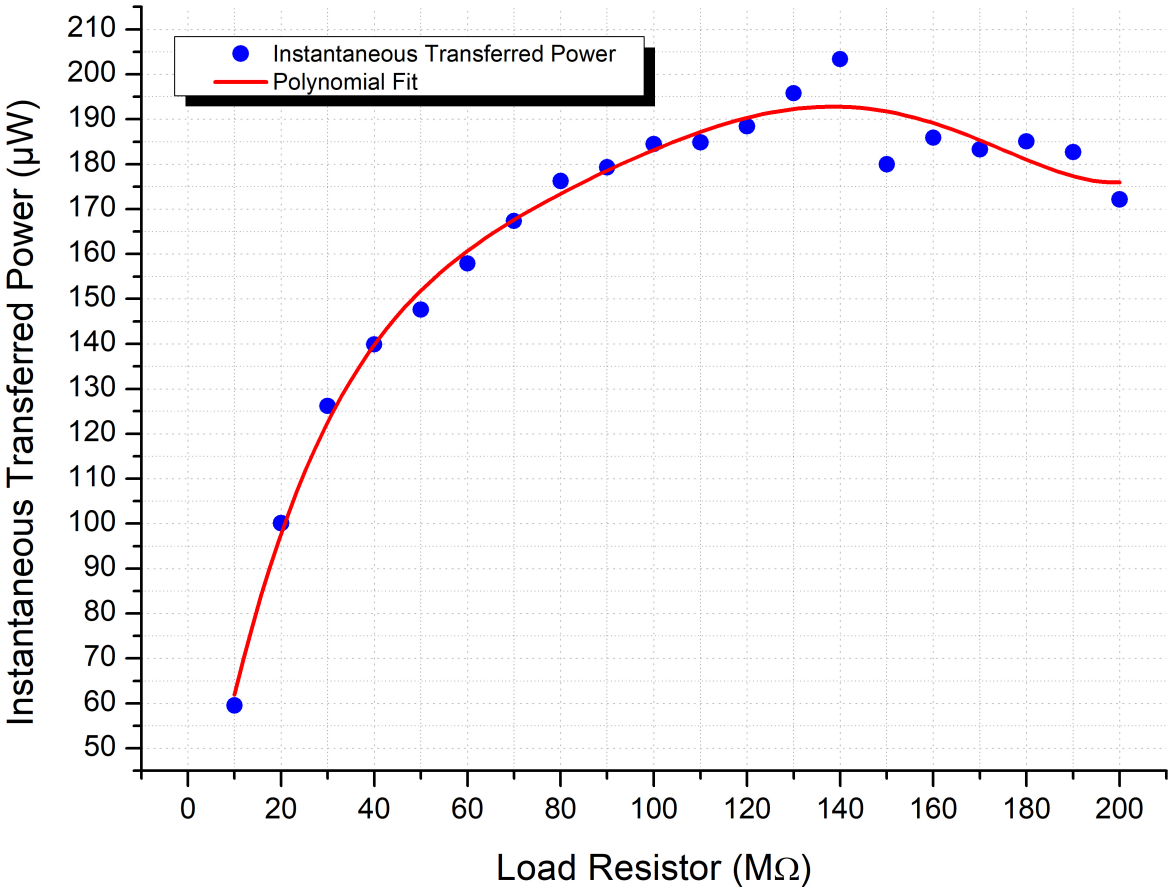

Figure 4.16. The instantaneous transferred power value for different load resistance for macro scale triboelectric harvester.



Figure 4.17. Driving LEDs with macro scale triboelectric generator.

4.4.1. Low Power Bluetooth Application

Bluetooth technology is a wireless connectivity protocol which provide a data transfer between different devices. This technology transfers data with lower power consumption with each new version. With the latest versions there is a new protocol which is named ultra low power bluetooth. Because of this feature, many IoT devices which uses this technology is commercially produced. These devices can perform their duty for a long time with only small batteries.

This study aims to show that the triboelectric generators can meet the energy requirements of data transmission with this technology and by showing that suggest a new path for a IoT devices which has no battery problems.

For this application, TI-CC2650 launchpad used as low power bluetooth chipset. This product can be seen in Figure 4.18. It is planned to operate the device only advertisement mode. In the advertisement mode it send a determined data package around periodically. In the application, the data package is planned as 18 bytes and time interval is 1 second.

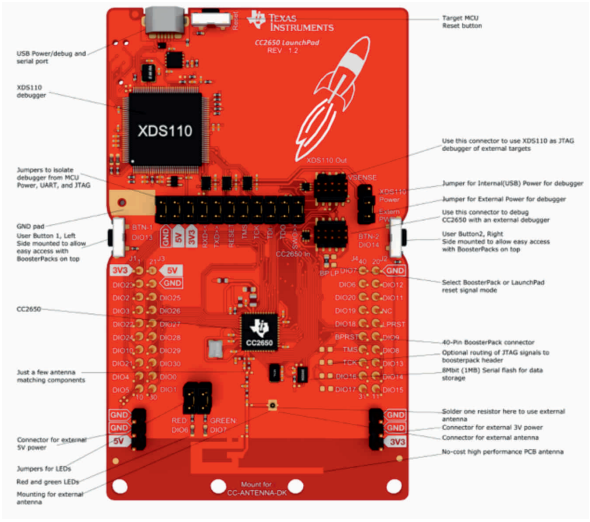

Figure 4.18. TI-CC2650 Launchpad [23].

In the previous works the power dissipations of this device for different settings are measured [24]. According to this study, the device in advertisement mode draws an average current of 7.61 μA at 3.3V. This means device dissipates a 25 μWs energy in a second. This means approximately 25 μJ energy is required for the transmission of 18 bytes data with low power bluetooth technology. In order to supply this energy the minimum 10μF capacitor is required. Since effective frequency of the triboelectric generator is approximately 5, the impedance of this capacitor is 3 kΩ. According to measurements, with this kind of load, there is almost no power transferred. Hence, it is clear that there is a need for a matching circuit.

In order to verify power measurements of the generator, test is applied with the 4 nF capacitor. It's impedance is approximately 8 MΩ. The capacitor is connected to TENG via full wave rectifier. During measurements, the charge collected in the capacitor is measured. For a one period of the contact and separation movement, the charge collected is measured as 200 nC. That means the capacitor is charged to 50 V and amount of energy transferred to capacitor is 5μJ. According to measurements data, the transferred energy at 10 MΩ is calculated as approximately 9μJ in one period. Since the 4 nF capacitor's impedance is lower than that it can be said it is consistent.

If the measurements data of macro scale triboelectric generator is investigated, the maximum energy transferred to load is calculated 33.2 μJ over a period. In order to do this calculation the load is connected to generator via full wave rectifier. Thus, if there is a matching circuit which transfer power from the matched capacitor to the required capacitor for application, the energy produced with triboelectric energy harvester is sufficient for the low power bluetooth applications. With matching circuit which has %75 efficiency, there can be IoT applications such as smart doormat.

5. CONCLUSIONS AND FUTURE WORK

In this study, three different triboelectric energy generator is designed, fabricated, and characterized. Device designs are made using contact mode structures. For all of the devices, dielectric material is used as one of the triboelectric layers, while a conductive material is used as other layer. In order to get high output power, triboelectric series are used to make material choice. By applying some modifications to selected materials, power output attempted to increase. Harvested energy from the fabricated devices are visualized in different applications.

On the first harvester, polydimethylsiloxane (PDMS) is used as negative material while the steel electrode used as positive. Then nano brushes created from polystyrene (PS) and poly(pentafluorostyrene) (PPFS) over PDMS are used as triboelectric layer. These nano structured surfaces with polymer brushes increase the transferred power significantly.

On the other harvesters, PTFE surface is used as triboelectric layer. Harvester which use a microfabricated steel electrode can be used as prototype of the keyboard button. This prototype can be used both as a sensor and as a harvester with its own energy. If more progress is made and several of them is integrated in one device, this prototype can be the first step of the completely batteryless keyboard system.

The triboelectric energy harvester manufactured as macro scale harvest a energy which is sufficient to lit up to approximately 200 commercial LED bulbs. It is showed that harvested energy can run the low power bluetooth applications. If it is thought that the low power bluetooth systems are used as data transmission system of many IoT applications, triboelectric energy harvesting method can be seen as a perfect candidate for use in these products.

The results achieved in this study is very promising in terms of future works. The harvested and transferred energy is adequate for many low power required applications and products. However, these products can have a different specifications. Because of this specifications, harvested energy may not be transferred efficiently. In order to solve this problem, design of the integrated circuits which transfer the power with a high efficiency can be suggested as a future work.

REFERENCES

1. Wang, Z. L., "Triboelectric nanogenerators as new energy technology and self-powered sensors – Principles, problems and perspectives", *Faraday Discuss.*, Vol. 176, pp. 447–458, 2014, http://dx.doi.org/10.1039/C4FD00159A.

2. Haydaroglu, I. and S. Mutlu, "Optical Power Delivery and Data Transmission in a Wireless and Batteryless Microsystem Using a Single Light Emitting Diode", *Journal of Microelectromechanical Systems*, Vol. 24, No. 1, pp. 155–165, February 2015.

3. Beeby, S., M. Tudor and N. White, "Energy harvesting vibration sources for microsystems applications", *Measurement Science and Technology*, Vol. 17, No. 12, pp. R175–R195, December 2006, https://eprints.soton.ac.uk/263645/.

4. Cook-Chennault, K. A., N. Thambi and A. M. Sastry, "Powering MEMS portable devices—a review of non-regenerative and regenerative power supply systems with special emphasis on piezoelectric energy harvesting systems", *Smart Materials and Structures*, Vol. 17, No. 4, p. 043001, 2008, http://stacks.iop.org/0964-1726/17/i=4/a=043001.

5. Beeby, S. P., R. N. Torah, M. J. Tudor, P. Glynne-Jones, T. O'Donnell, C. R. Saha and S. Roy, "A micro electromagnetic generator for vibration energy harvesting", *Journal of Micromechanics and Microengineering*, Vol. 17, No. 7, p. 1257, 2007, http://stacks.iop.org/0960-1317/17/i=7/a=007.

6. Miyazaki, M., H. Tanaka, G. Ono, T. Nagano, N. Ohkubo, T. Kawahara and K. Yano, "Electric-energy Generation Using Variable-capacitive Resonator for Power-free LSI: Efficiency Analysis and Fundamental Experiment", *Proceedings of the 2003 International Symposium on Low Power Electronics and Design*, ISLPED '03, pp. 193–198, ACM, New York, NY, USA, 2003, http://doi.acm.org/10.1145/871506.871555.

7. Roundy, S. J., *Energy scavenging for wireless sensor nodes with a focus on vibration to electricity conversion*, Ph.D. Thesis, University of California, Berkeley Berkeley, CA, 2003.

8. Roundy, S., P. K. Wright and J. Rabaey, "A study of low level vibrations as a power source for wireless sensor nodes", *Computer Communications*, Vol. 26, No. 11, pp. 1131 – 1144, 2003, http://www.sciencedirect.com/science/article/pii/S0140366402002487.

9. Vives, A. A., *Piezoelectric Transducers and Applications*, Springer, Berlin, Heidelberg, 2004.

10. Deng, L., Z. Wen, X. Zhao, C. Yuan, G. Luo and J. Mo, "High Voltage Output MEMS Vibration Energy Harvester ind_{31}Mode With PZT Thin Film", *Journal of Microelectromechanical Systems*, Vol. 23, No. 4, pp. 855–861, August 2014.

11. Zhu, G., J. Chen, T. Zhang, Q. Jing and Z. L. Wang, "Radial-arrayed rotary electrification for high performance triboelectric generator", *Nature communications*, Vol. 5, p. 3426, 2014.

12. Baytekin, H., A. Patashinski, M. Branicki, B. Baytekin, S. Soh and B. A. Grzybowski, "The mosaic of surface charge in contact electrification", *Science*, p. 1201512, 2011.

13. Tang, W., T. Jiang, F. R. Fan, A. F. Yu, C. Zhang, X. Cao and Z. L. Wang, "Liquid-metal electrode for high-performance triboelectric nanogenerator at an instantaneous energy conversion efficiency of 70.6%", *Advanced Functional Materials*, Vol. 25, No. 24, pp. 3718–3725, 2015.

14. McCarty, L. S. and G. M. Whitesides, "Electrostatic charging due to separation of ions at interfaces: contact electrification of ionic electrets", *Angewandte Chemie International Edition*, Vol. 47, No. 12, pp. 2188–2207, 2008.

15. Wang, Z. L., "Triboelectric nanogenerators as new energy technology for self-powered systems and as active mechanical and chemical sensors", *ACS nano*, Vol. 7, No. 11, pp. 9533–9557, 2013.

16. Diaz, A. and R. Felix-Navarro, "A semi-quantitative tribo-electric series for polymeric materials: the influence of chemical structure and properties", *Journal of Electrostatics*, Vol. 62, No. 4, pp. 277–290, 2004.

17. Davies, D. K., "Charge generation on dielectric surfaces", *Journal of Physics D: Applied Physics*, Vol. 2, No. 11, p. 1533, 1969, http://stacks.iop.org/0022-3727/2/i=11/a=307.

18. Gokdel, Y., B. Sarioglu, S. Mutlu and A. Yalcinkaya, "Design and fabrication of two-axis micromachined steel scanners", *Journal of Micromechanics and Microengineering*, Vol. 19, No. 7, p. 075001, 2009.

19. Gokdel, Y. D., S. Mutlu and A. D. Yalcinkaya, "Self-terminating electrochemical etching of stainless steel for the fabrication of micro-mirrors", *Journal of Micromechanics and Microengineering*, Vol. 20, No. 9, p. 095009, 2010.

20. Iseri, E., K. O. Ulgen, C. Yilmaz and S. Mutlu, "Fabrication of steel displacement amplifiers integrated to microfluidic channels", *Micro Electro Mechanical Systems (MEMS), 2016 IEEE 29th International Conference on*, pp. 493–496, IEEE, 2016.

21. Iseri, E. and S. Mutlu, "Realization of triboelectric energy harvesters using steel-polymer microfabrication methods", *Micro Electro Mechanical Systems (MEMS), 2017 IEEE 30th International Conference on*, pp. 817–820, IEEE, 2017.

22. Niu, S., S. Wang, L. Lin, Y. Liu, Y. S. Zhou, Y. Hu and Z. L. Wang, "Theoretical study of contact-mode triboelectric nanogenerators as an effective power source", *Energy & Environmental Science*, Vol. 6, No. 12, pp. 3576–3583, 2013.

23. Instruments, T., *CC26x0 SimpleLink™ Bluetooth® low*

energy Software Stack 2.2.x Developer's Guide, 2010, `http://www.ti.com/lit/ug/swru393e/swru393e.pdf`, accessed at August 2018.

24. Şerbetci, C., "*Low power RF communication hardware for IoT*", Senior Design Project, Boğaziçi University, 2017.